Tomography of the Mojavian Lithosphere Viscosity from Space Geodetic data of the Landers and Hector Mine Earthquakes

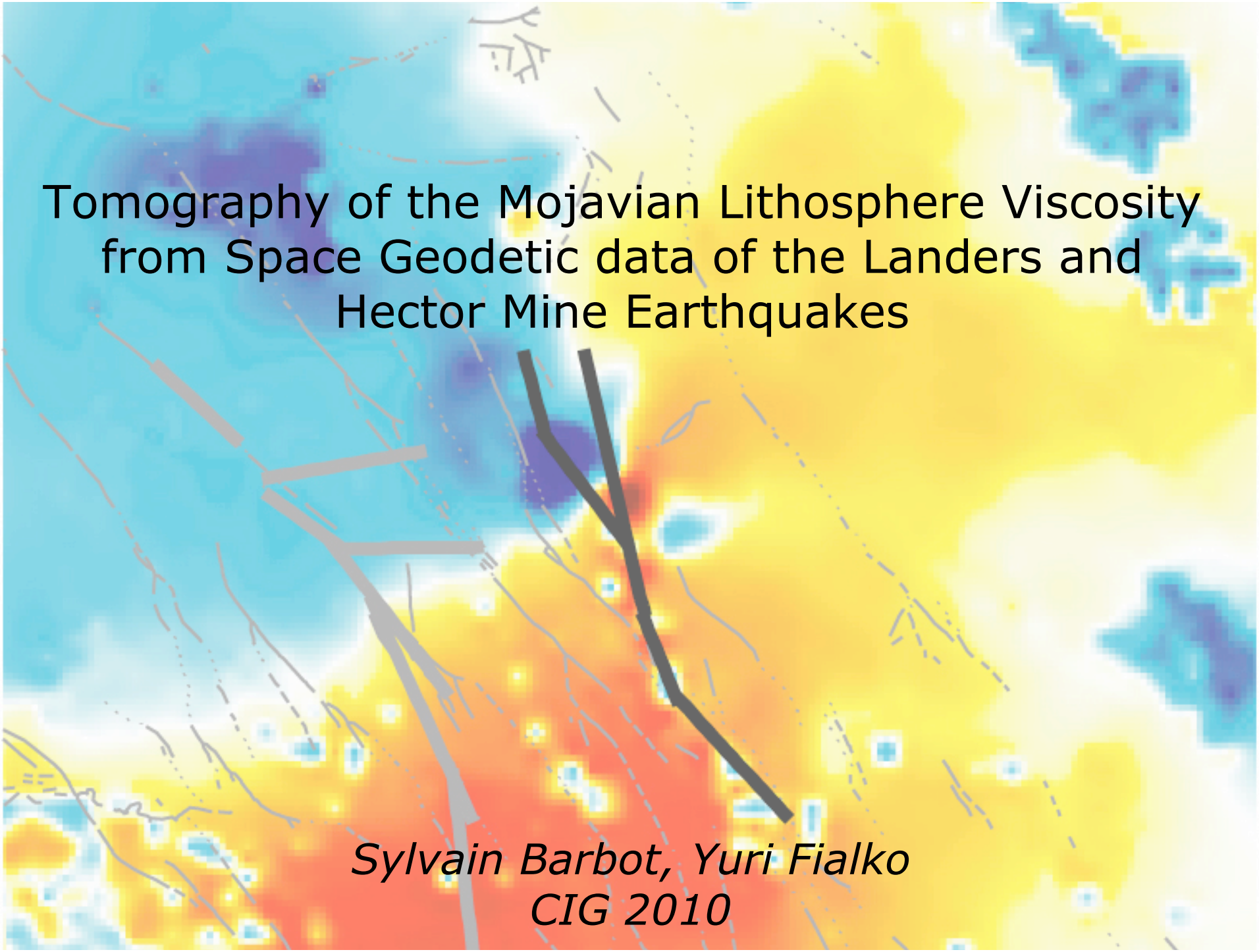

Sylvain Barbot, Yuri Fialko

CIG 2010

Poroelastic rebound along the Landers 1992 earthquake surface rupture

Gilles Peltzer, Paul Rosen, and Francois Rogez
Jet Propulsion Laboratory, California Institute of Technology, Pasadena

K. Hudnut
U.S. Geological Survey, Pasadena, California

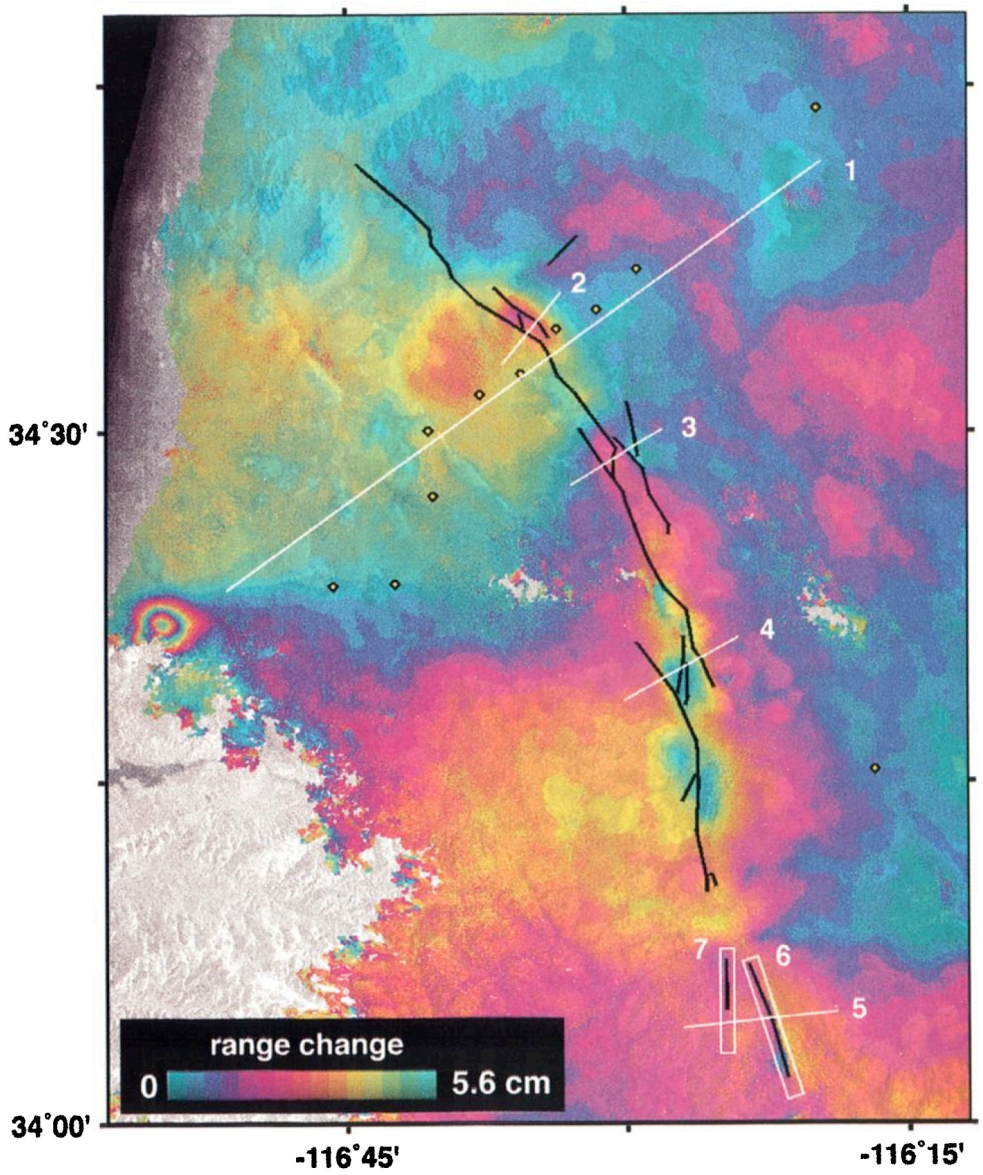

Modeling afterslip and aftershocks following the 1992 Landers earthquake

H. Perfettini[1] and J.-P. Avouac[2]

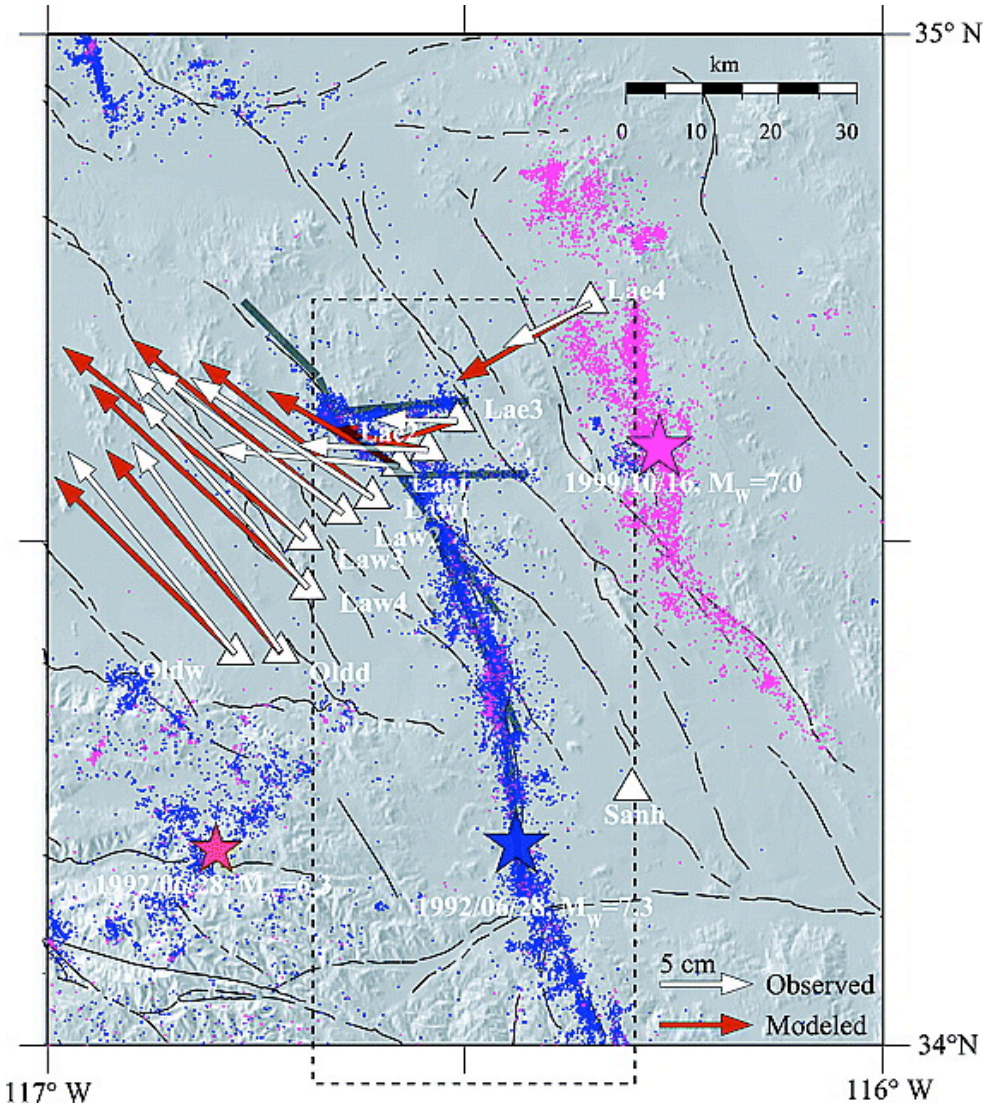

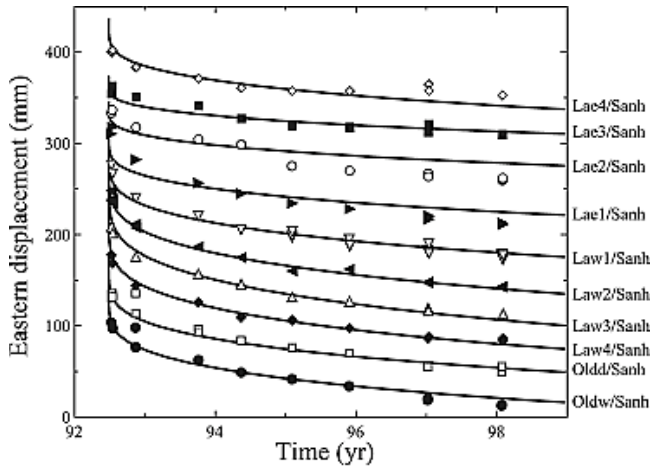

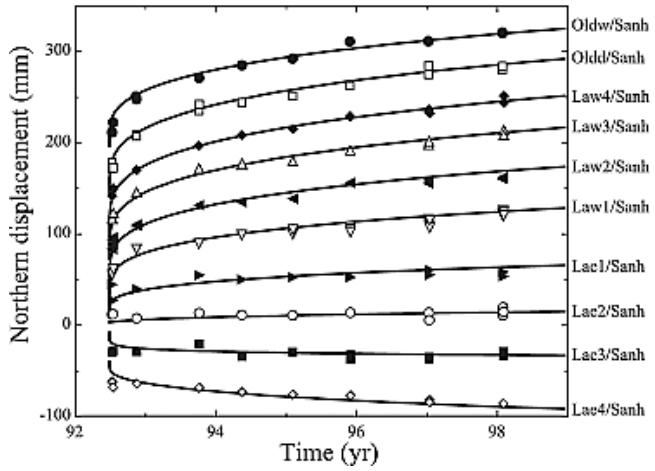

Viscoelastic Flow in the Lower Crust after the 1992 Landers, California, Earthquake

Jishu Deng,* Michael Gurnis, Hiroo Kanamori, Egill Hauksson

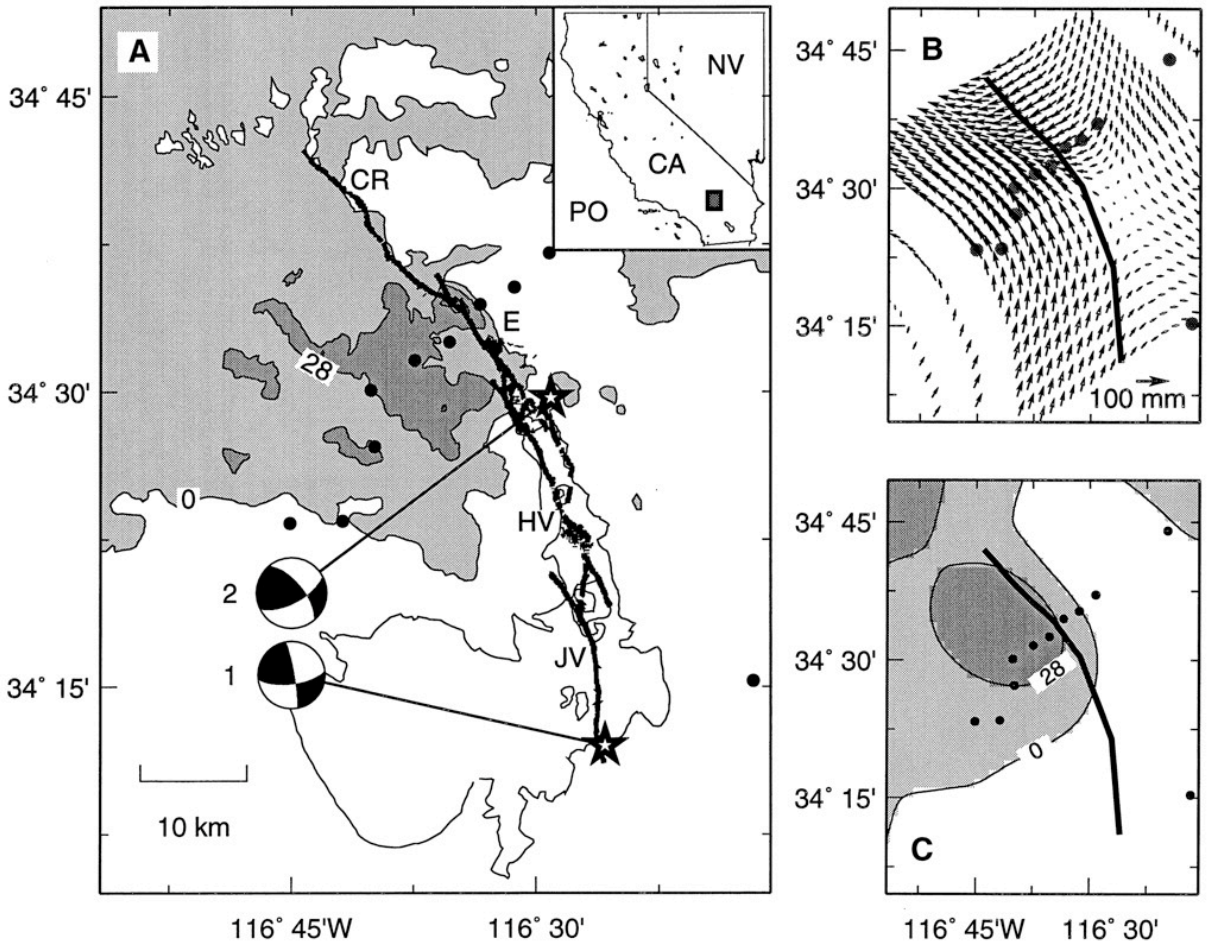

Evidence of fluid-filled upper crust from observations of postseismic deformation due to the 1992 M_w7.3 Landers earthquake

Yuri Fialko

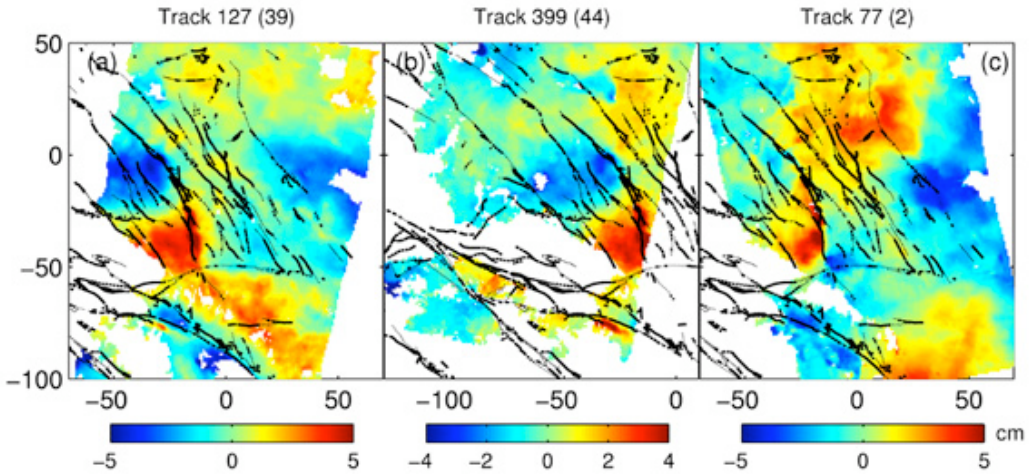

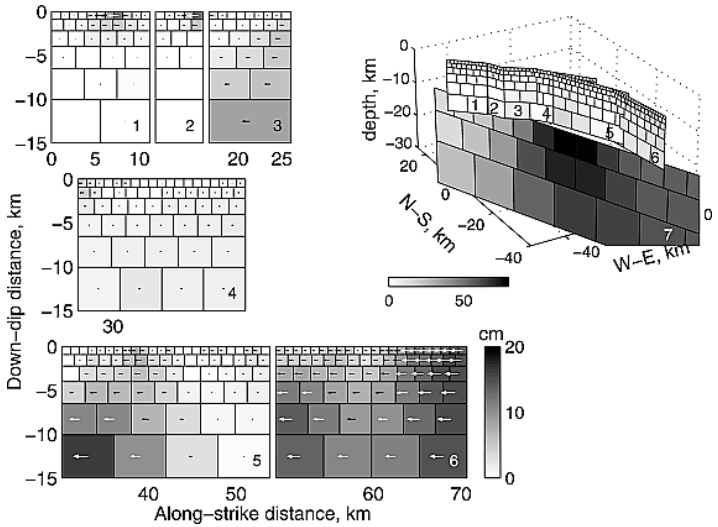

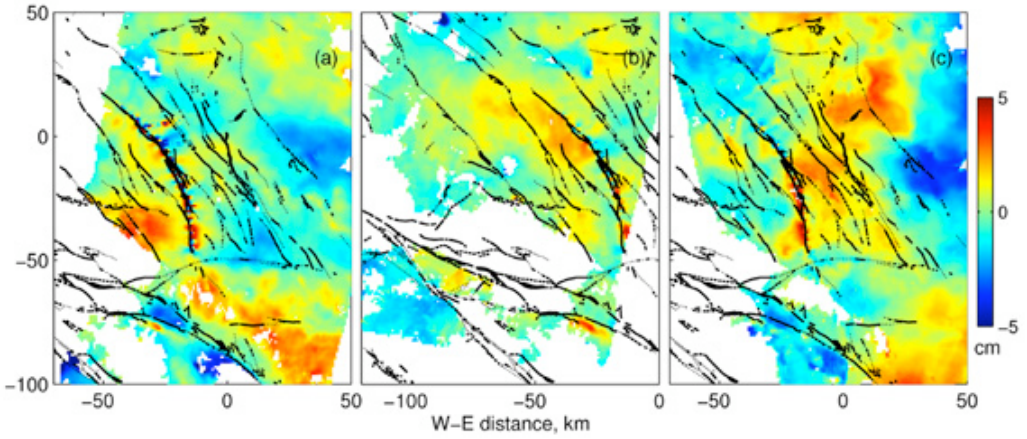

Mantle Flow Beneath a Continental Strike-Slip Fault: Postseismic Deformation After the 1999 Hector Mine Earthquake

Fred F. Pollitz,* Chuck Wicks, Wayne Thatcher

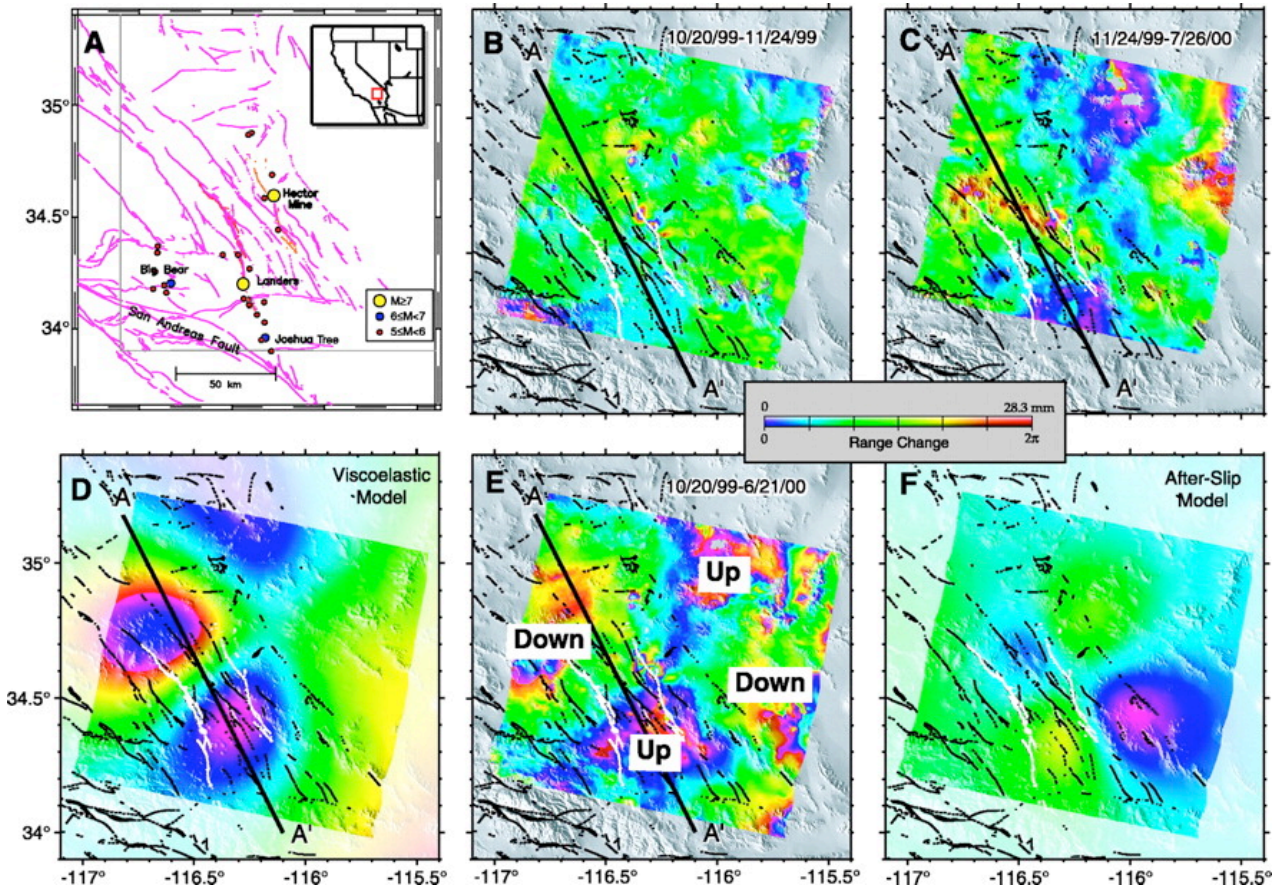

Far-reaching transient motions after Mojave earthquakes require broad mantle flow beneath a strong crust

Andrew M. Freed,[1] Roland Bürgmann,[2] and Thomas Herring[3]

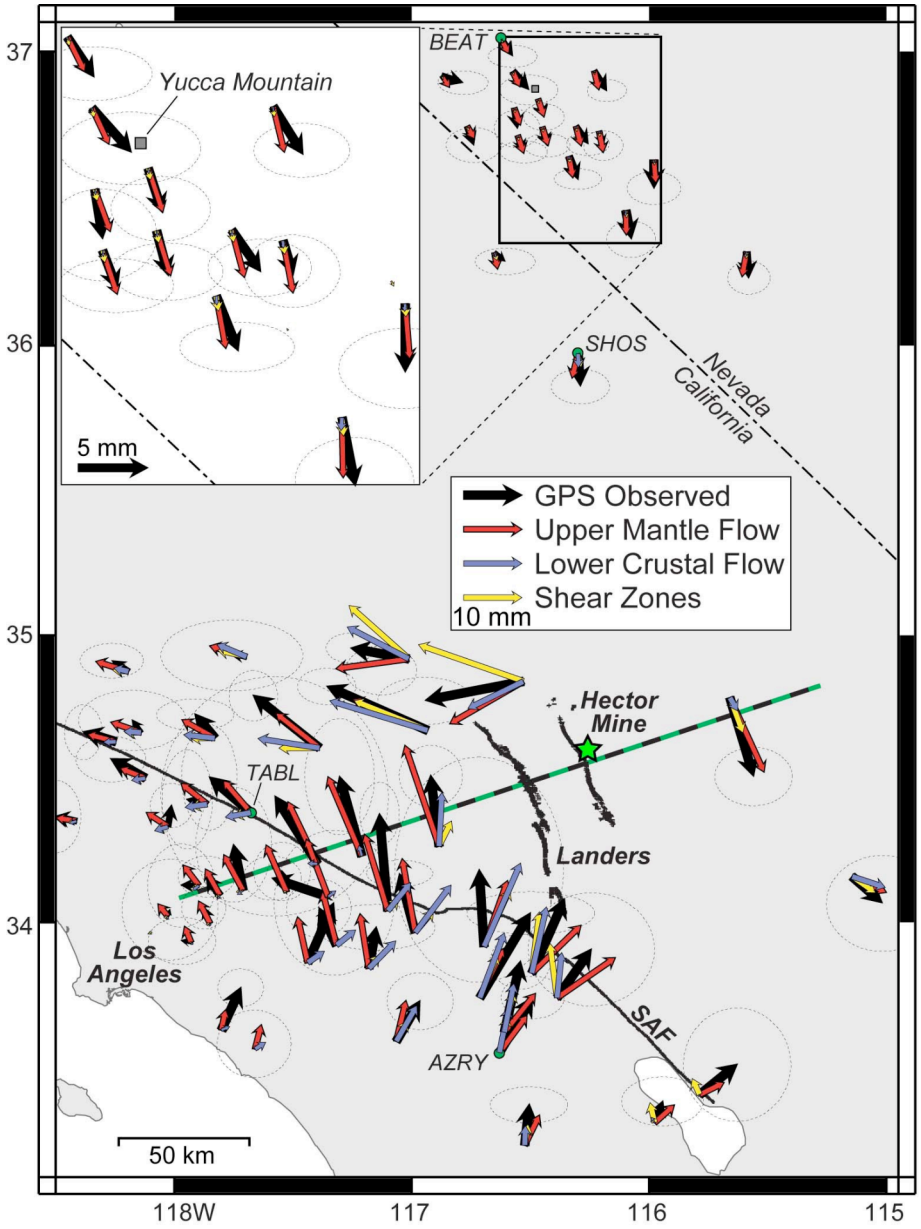

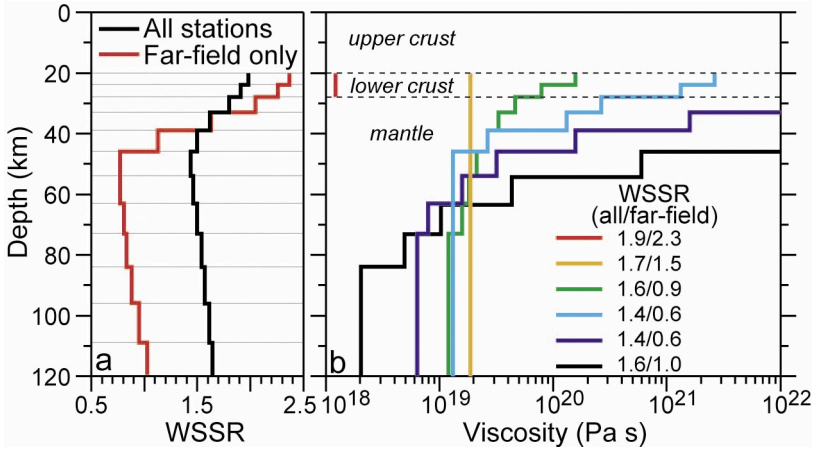

Evidence of power-law flow in the Mojave desert mantle

Andrew M. Freed[1] & Roland Bürgmann[2]

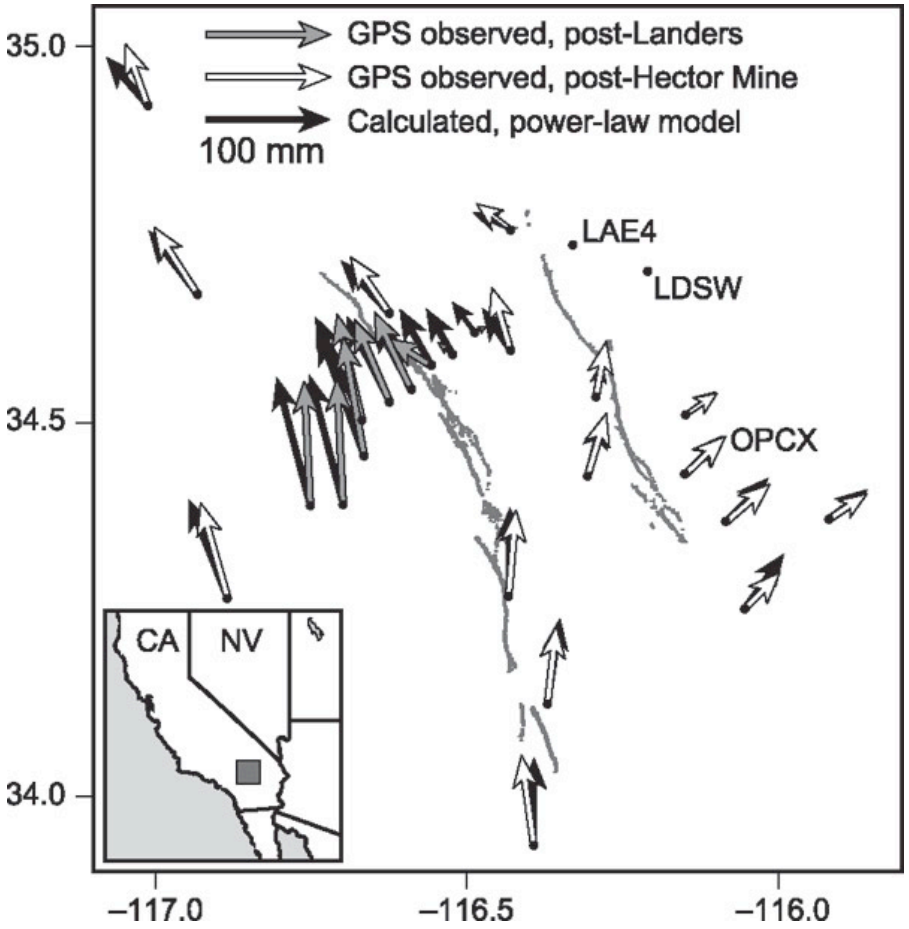

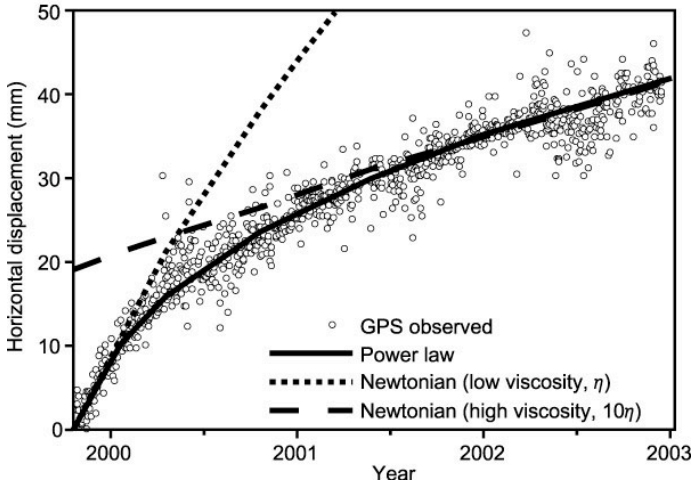

Time dependence of post Hector Mine GPS displacements favors a **nonlinear** ductile rheology.

A. GPS and modeled horizontal displacements

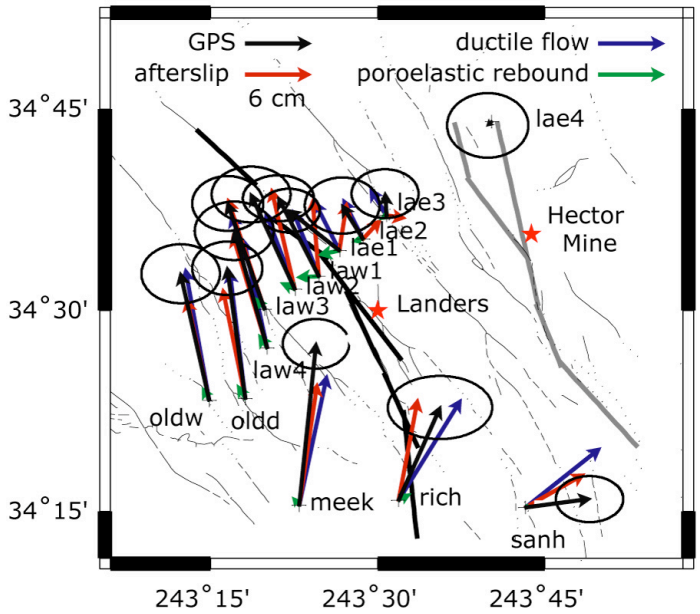

B. Afterslip model h= 15 km

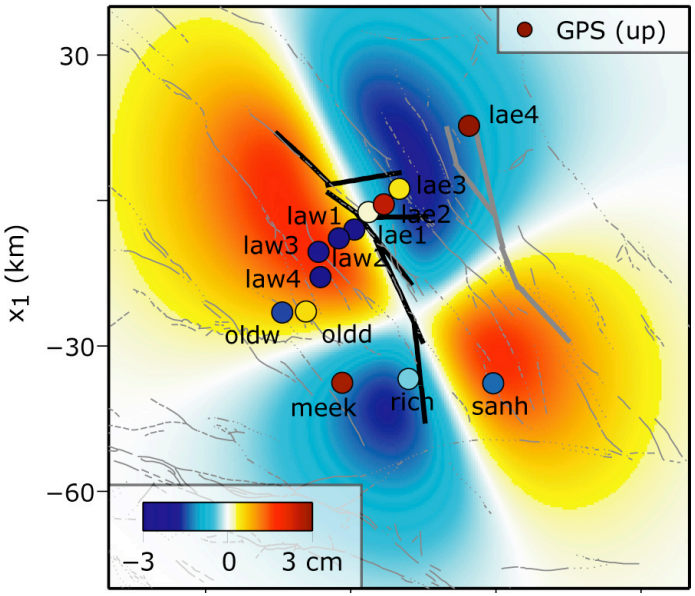

C. Crème brûlée linear model H = 40 km

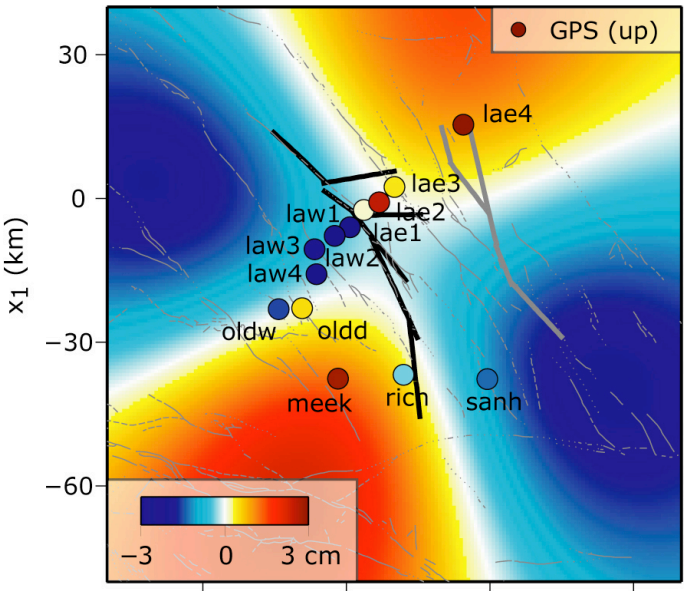

D. Poroelastic rebound model

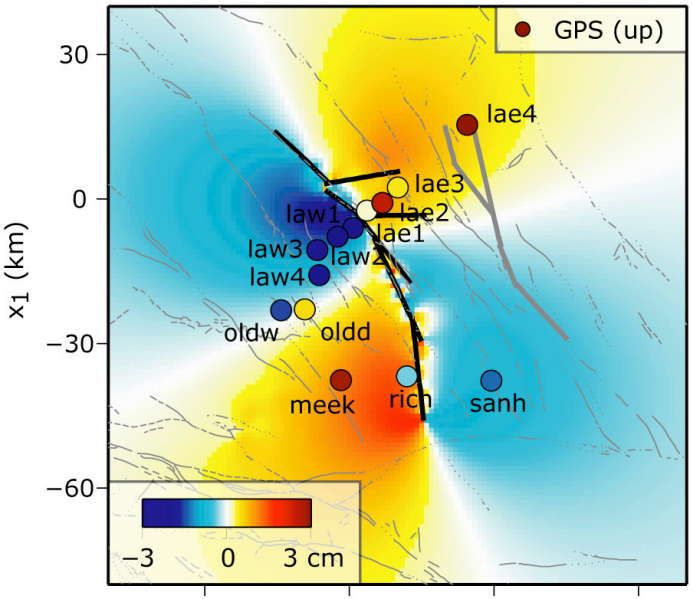

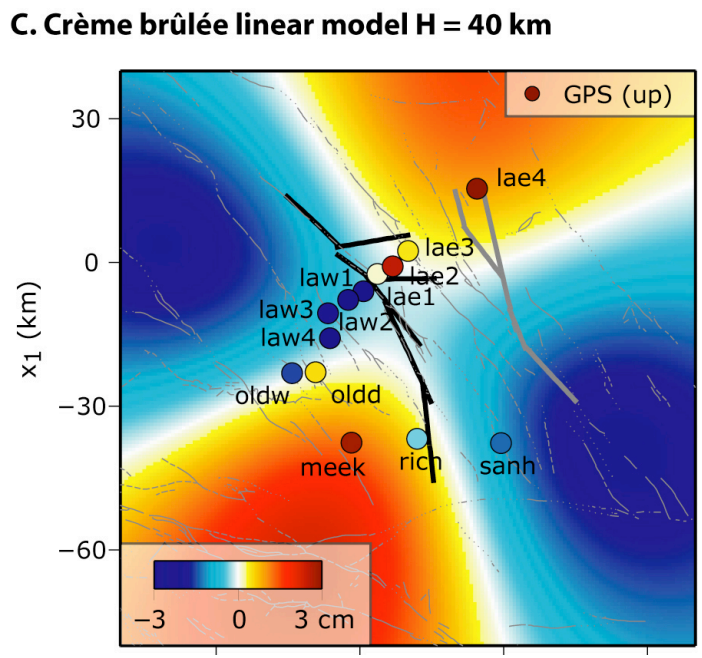
C. Crème brûlée linear model H = 40 km
GPS (up)
lae4
lae3
law1
lae2
lae1
law3
law2
law4
oldw
oldd
meek
rich
sanh
−3
0
3 cm
30
0
−30
−60
x1 (km)

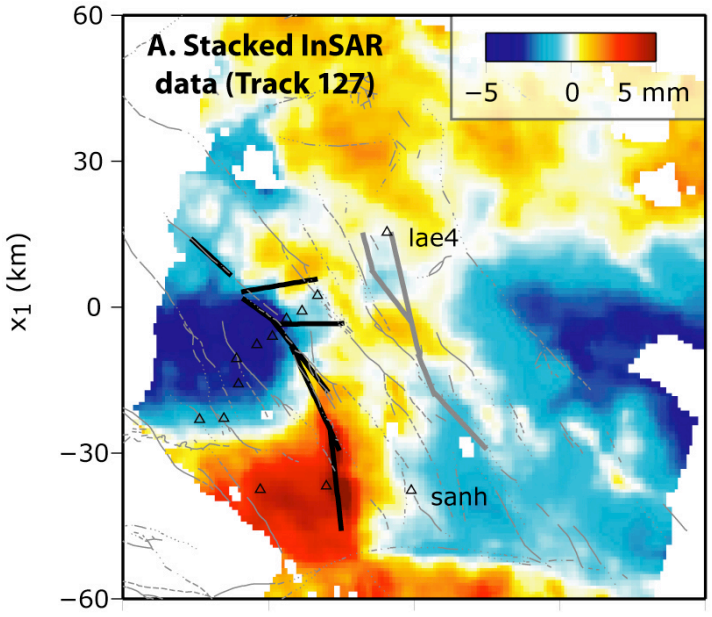
A. Stacked InSAR data (Track 127)
−5
0
5 mm
lae4
sanh
30
0
−30
−60
x1 (km)

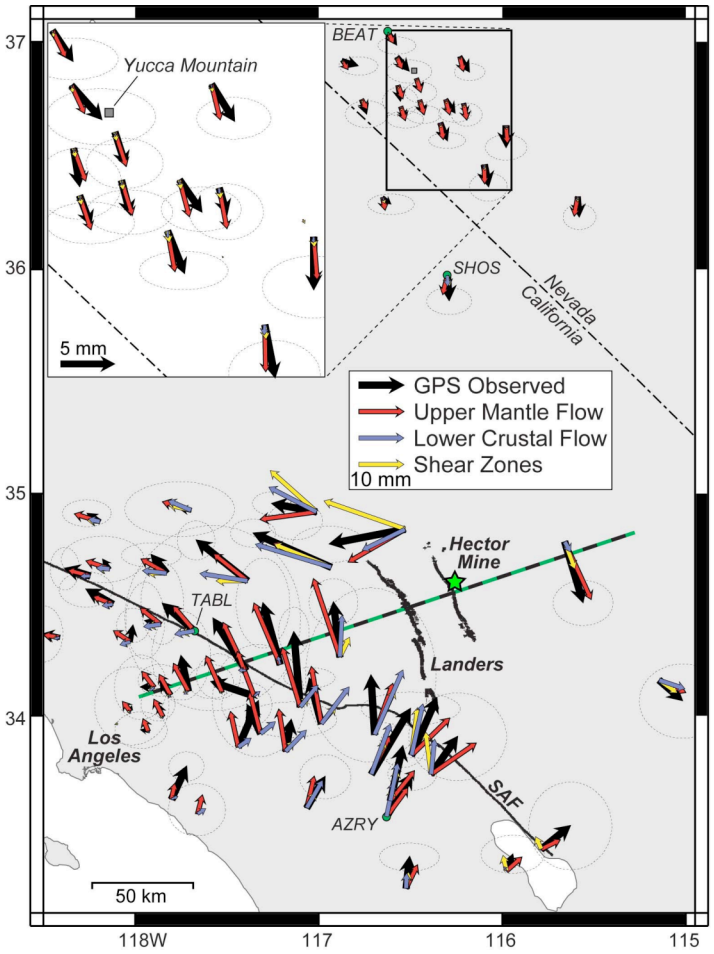
Yucca Mountain
BEAT
SHOS
Nevada
California
5 mm
GPS Observed
Upper Mantle Flow
Lower Crustal Flow
Shear Zones
10 mm
Hector Mine
TABL
Landers
Los Angeles
AZRY
SAF
50 km
37
36
35
34
118W
117
116
115

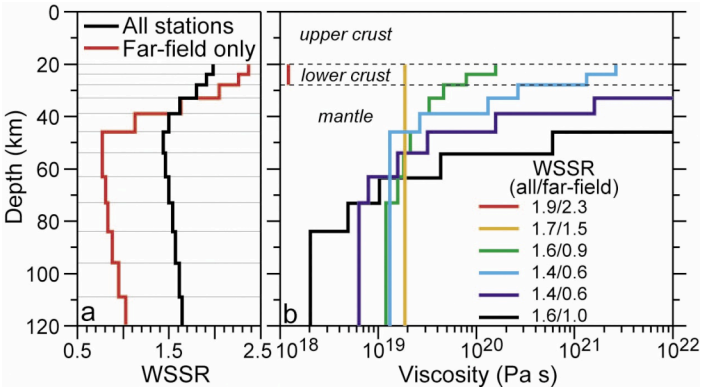
All stations
Far-field only
upper crust
lower crust
mantle
WSSR
(all/far-field)
1.9/2.3
1.7/1.5
1.6/0.9
1.4/0.6
1.4/0.6
1.6/1.0
Depth (km)
a
b
WSSR
Viscosity (Pa s)

Outlines

- Design of the linear inverse problem
- Models of post-Landers deformation with InSAR data
  - afterslip transitioning to viscous flow
  - poroelastic rebound & viscous flow
  - viscoelastic flow alone
- Resolution of geodetic data
- Models of post-Hector Mine deformation with InSAR and GPS data
  - poroelastic rebound & viscous flow
  - viscoelastic flow alone
- Lateral variations in viscosity
- Conclusions

Outlines

- Design of the linear inverse problem
- Models of post-Landers deformation with InSAR data
  - afterslip transitioning to viscous flow
  - poroelastic rebound & viscous flow
  - viscoelastic flow alone
- Resolution of geodetic data
- Models of post-Hector Mine deformation with InSAR and GPS data
  - poroelastic rebound & viscous flow
  - viscoelastic flow alone
- Lateral variations in viscosity
- Conclusions

Design of inverse problem: the rheology

- Aseismic creep rheology: rate-strengthening friction

$$\dot{s} = 2\dot{s}_0 \sinh\frac{\tau}{a\sigma} \qquad t_c = \frac{a\sigma}{\dot{s}_0}\frac{L}{G}$$

- Viscoelastic flow: power-law rheology

$$\dot{\varepsilon} = A\left(\frac{\tau}{G}\right)^n \qquad t_m = \frac{1}{A} \quad for \quad n = 1$$

- Poroelastic rebound: full relaxation

$$K_d = (1-\beta)K_u$$

no time scale

A Unified Continuum Representation of Postseismic Relaxation Mechanisms: Semi-Analytic Models of Afterslip, Poroelastic Rebound and Viscoelastic Flow

Sylvain Barbot*, Yuri Fialko www.its.caltech.edu/~sbarbot/crust/

Design of inverse problem: misfit reduction by exploration of parameter

Mantle Flow Beneath a Continental Strike-Slip Fault: Postseismic Deformation After the 1999 Hector Mine Earthquake

Fred F. Pollitz,* Chuck Wicks, Wayne Thatcher

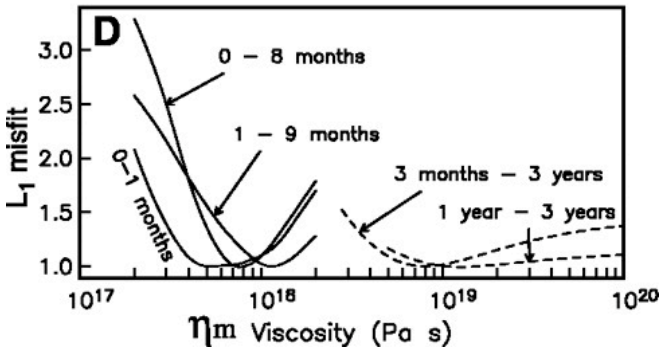

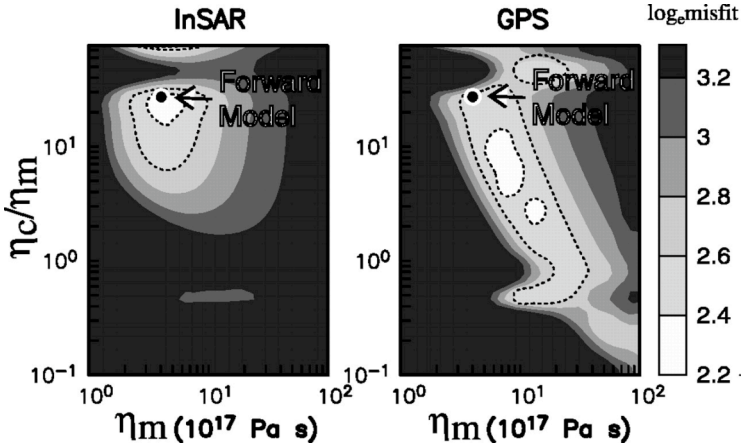

Pore fluid diffusion:
not time-space separable

Far-reaching transient motions after Mojave earthquakes require broad mantle flow beneath a strong crust

Andrew M. Freed,[1] Roland Bürgmann,[2] and Thomas Herring[3]

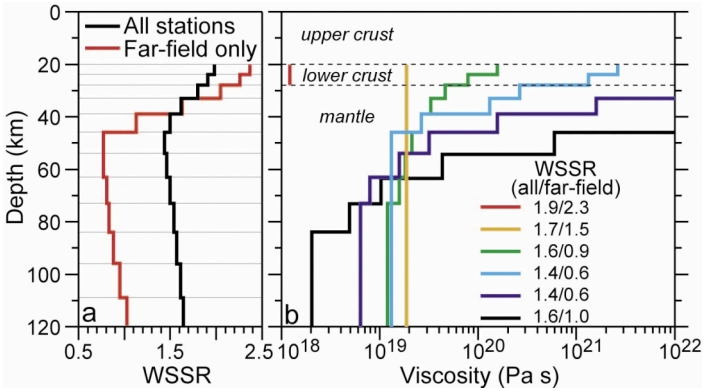

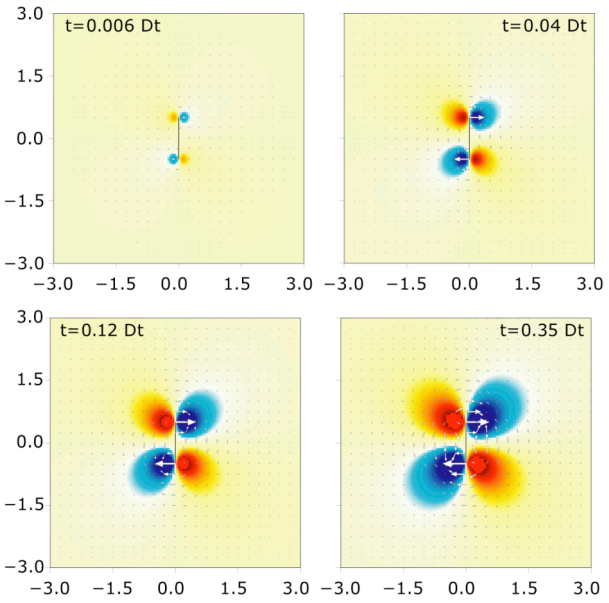

Design of inverse problem: a linear solution?

A. Dominant mode of post-Landers LOS deformation

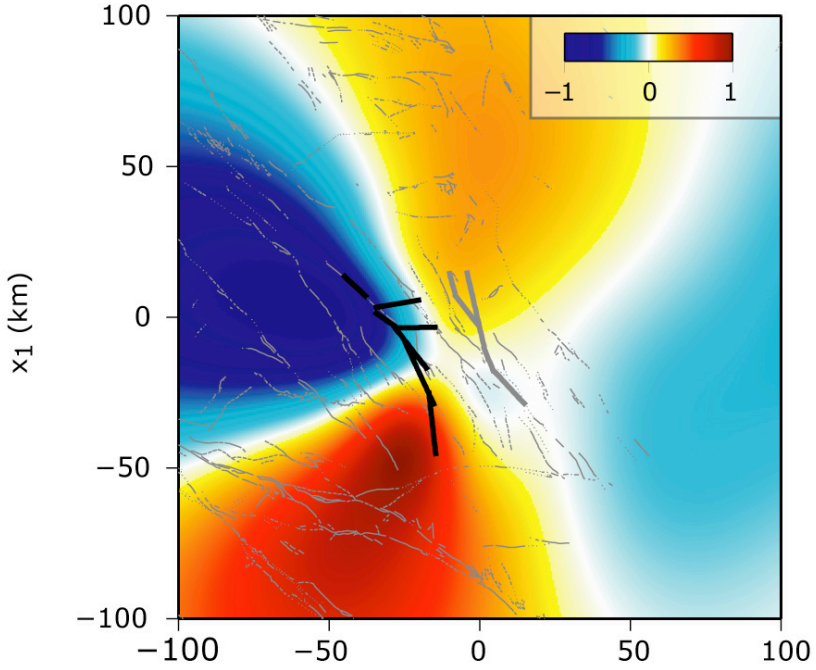

B. Second dominant mode of post-Landers LOS deformation

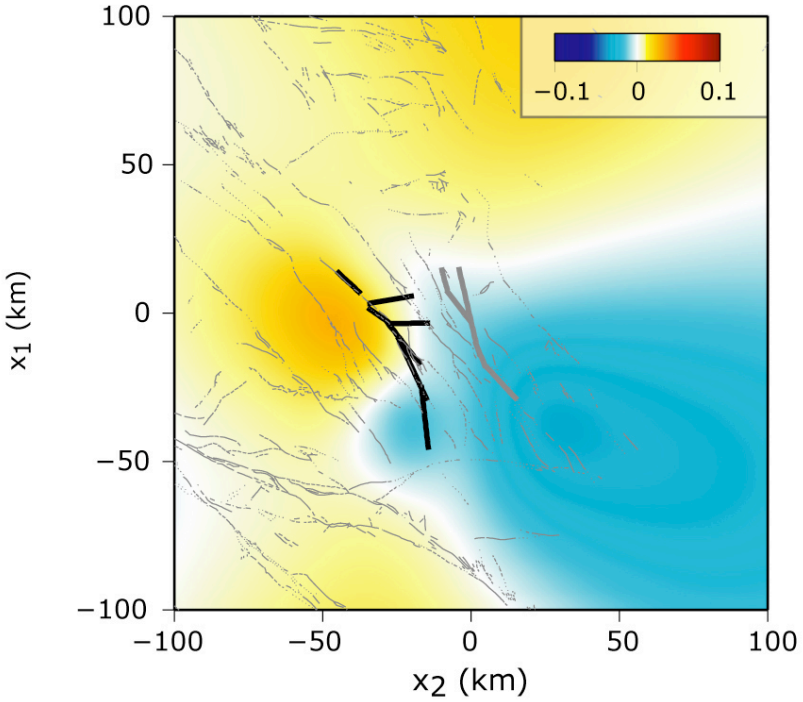

C. Time dependence of post-Landers deformation modes

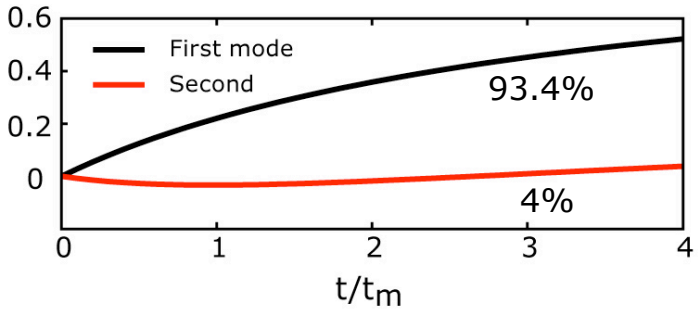

Post-Landers viscoelastic relaxation in the radar line of sight (LOS) is dominated by a time-space separable signal.

Design of inverse problem: a linear solution?

D. Dominant mode of poroelastic LOS deformation

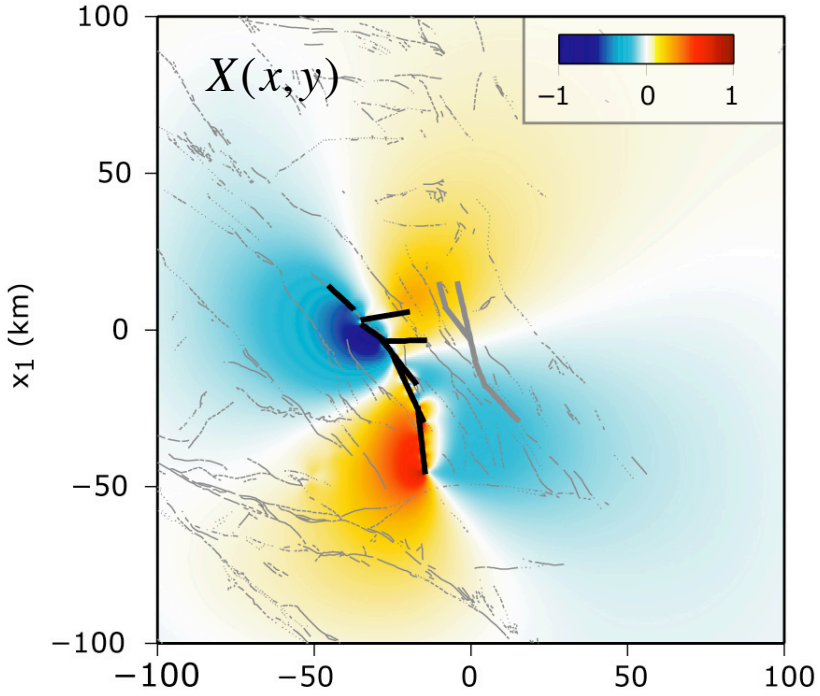

Full poroelastic rebound is separable in amplitude and spatial distribution.

$$LOS(x,y;\beta) = B(\beta)X(x,y)$$

F. Fluid/solid coupling dependence of modes

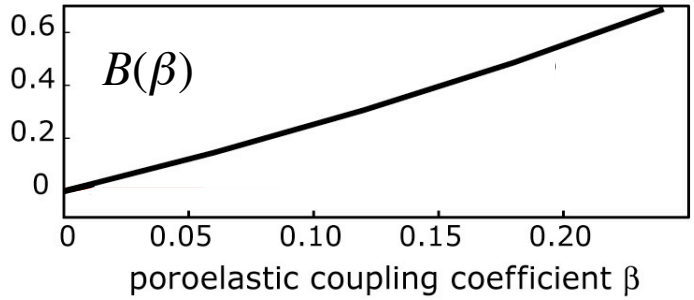

Design of inverse problem: a linear inverse problem

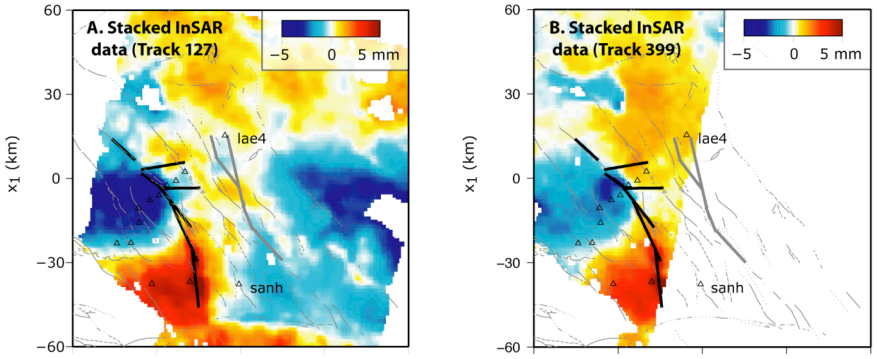

data vector

response of a nominal flow in horizon *i*

$$\mathbf{d} = \begin{bmatrix} d_1 \\ \vdots \\ d_N \end{bmatrix} \qquad \mathbf{G} = \begin{bmatrix} G_{11} & \cdots & \cdots & \cdots & \cdots & \cdots & G_{1M} \\ \vdots & & & & & & \vdots \\ G_{N1} & \cdots & \cdots & \cdots & \cdots & \cdots & G_{NM} \end{bmatrix} \qquad \mathbf{m} = \begin{bmatrix} m_1 \\ \vdots \\ m_M \end{bmatrix}$$

amplitude of deformation for horizon *i*

inversion

minimize the misfit

$$\chi = \|\mathbf{d} - \mathbf{Gm}\|$$

with non-negativity constraint

$$\mathbf{Am} \geq 0$$

and regularization

$$\lambda^2 \, \mathbf{Dm} = 0$$

include a bilinear function to compensate for imprecise knowledge of orbits.

Outlines

- Design of the linear inverse problem
- Models of post-Landers deformation with InSAR data
  - afterslip transitioning to viscous flow
  - poroelastic rebound & viscous flow
  - viscoelastic flow alone
- Resolution of geodetic data
- Models of post-Hector Mine deformation with InSAR and GPS data
  - poroelastic rebound & viscous flow
  - viscoelastic flow alone
- Lateral variations in viscosity
- Conclusions

Schizosphere model

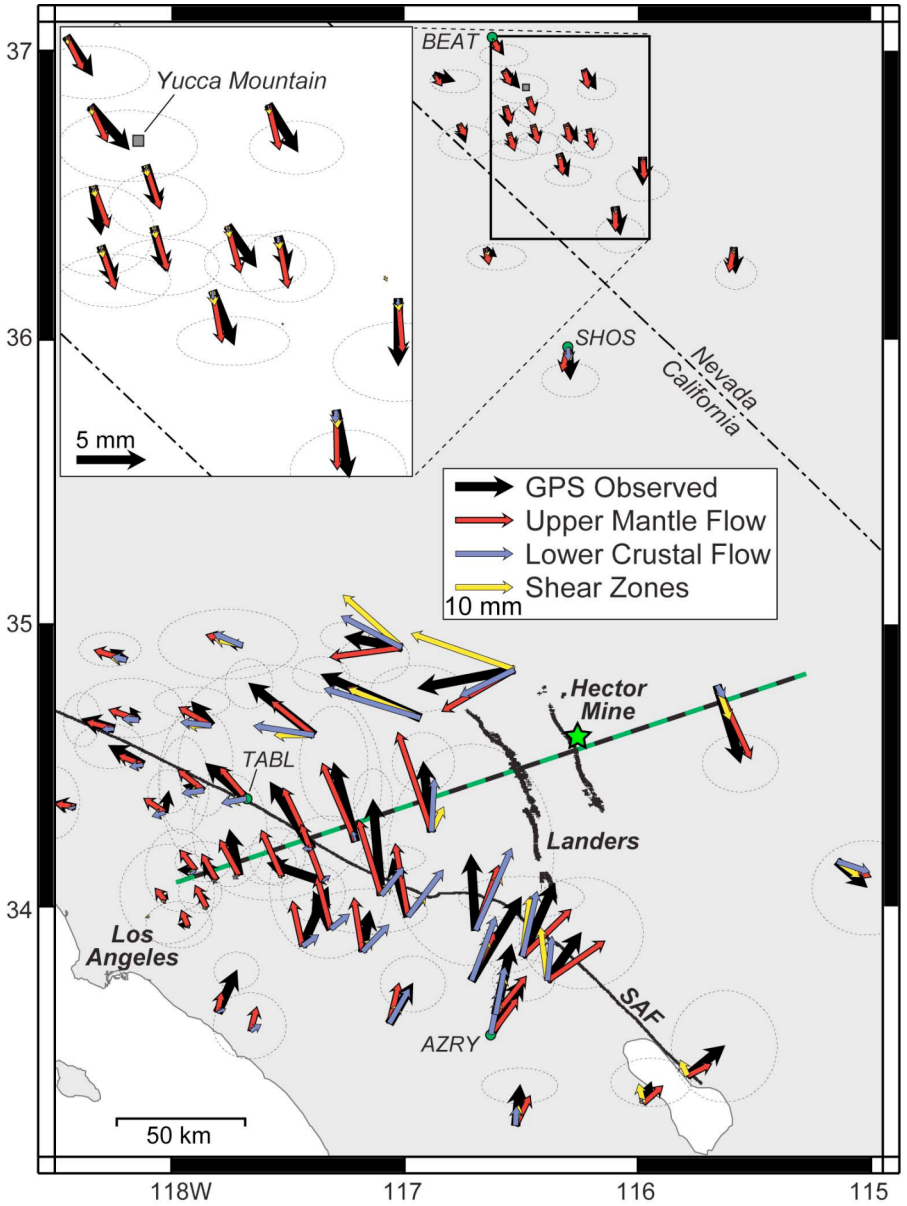

Freed et al., 2007

Displacement on far-field Nevada GPS stations requires **deep sources** of deformation.

How deep is the viscous substrate if deformation is accomodated by **mylonitic shear** in the **schizosphere**?

Crème-brûlée model **schizosphere model**

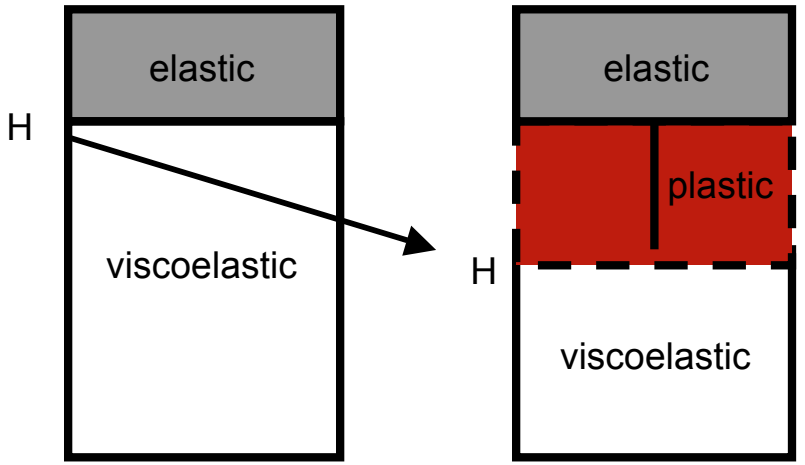

Schizosphere model

crème-brûlée models

schizosphere models

H = 30 km

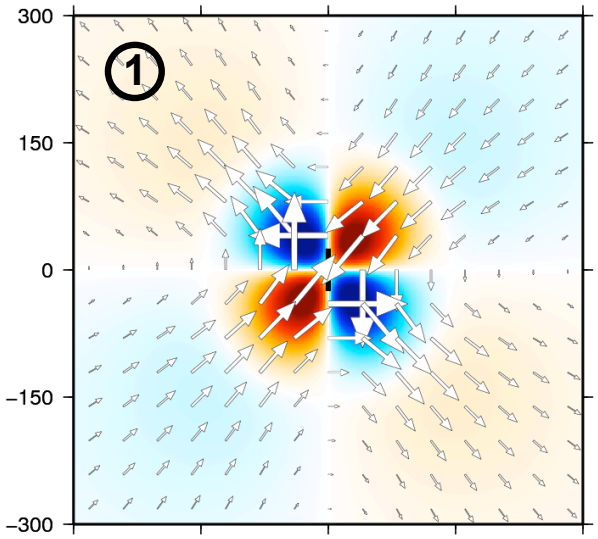

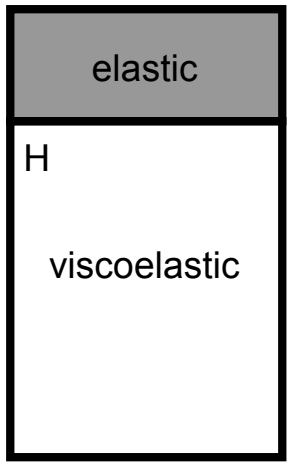

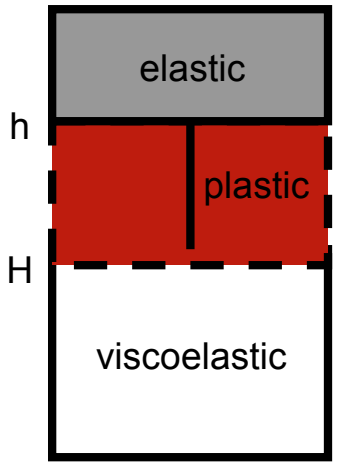

h = 15 km; H = 40 km

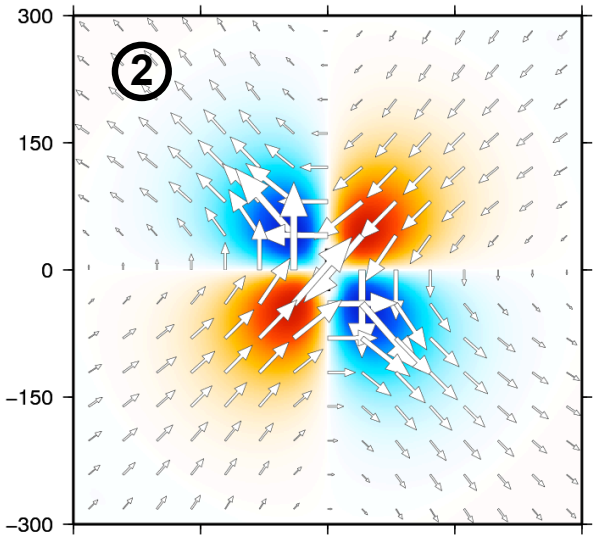

H = 50 km

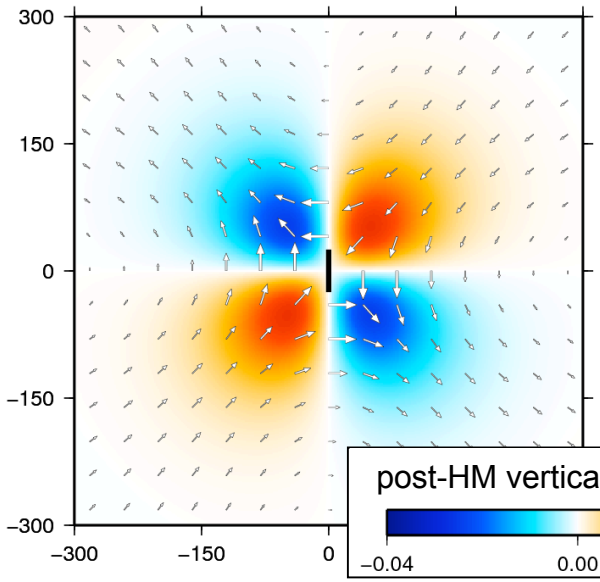

The **brittle-ductile transition** depth may be located 20 km deeper than in crème-brûlée models if shear stress is guided along **weak fault roots**.

Thin **crème-brûlée** and **thick-schizosphere** models produce similar far-field horizontal displacements.

h = 15 km; H = 50 km

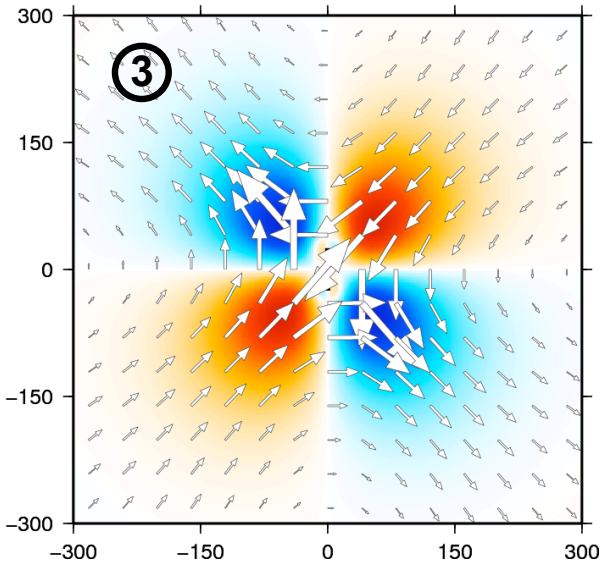

Afterslip + viscous flow model

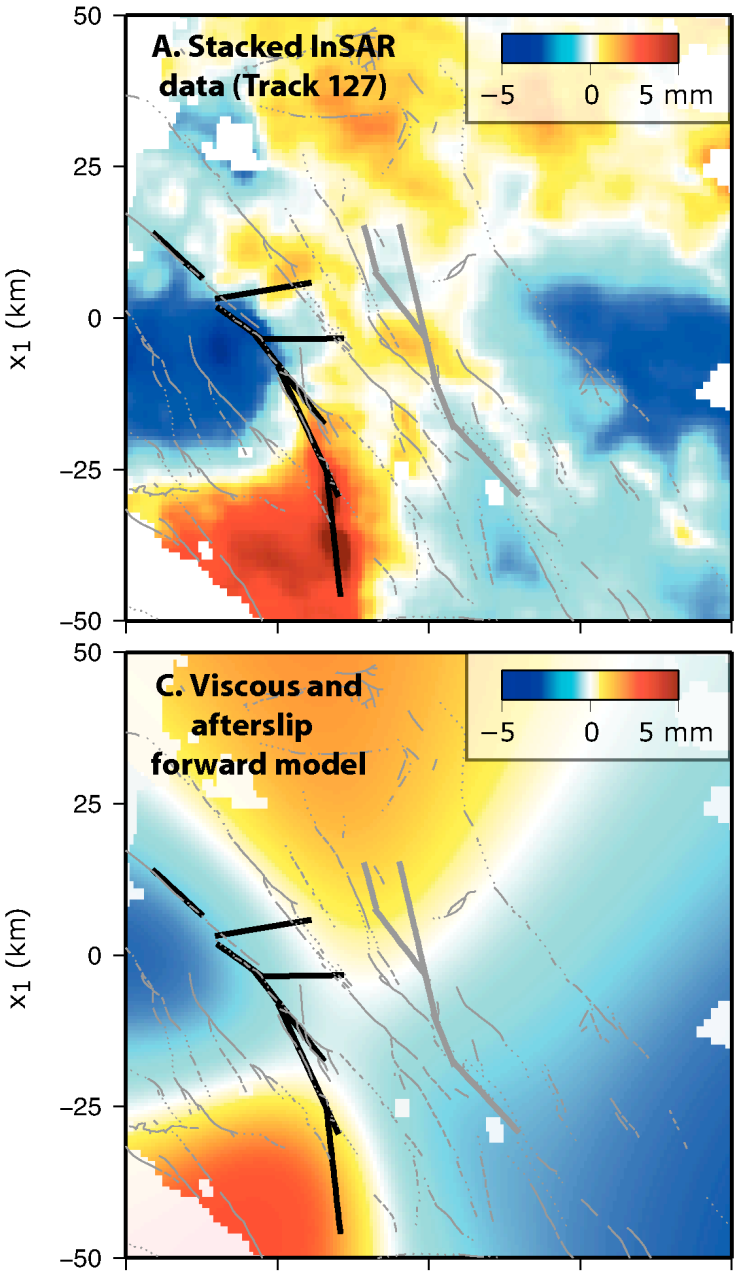

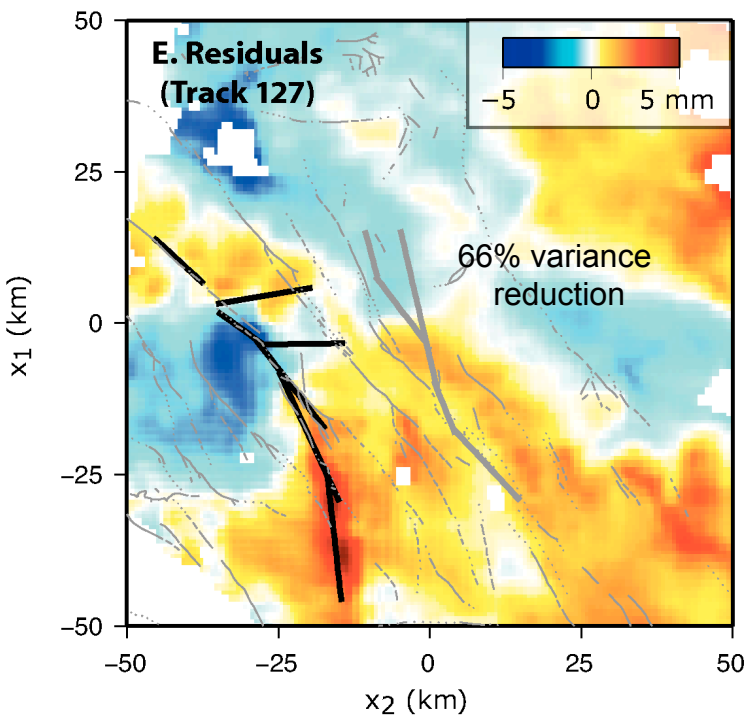

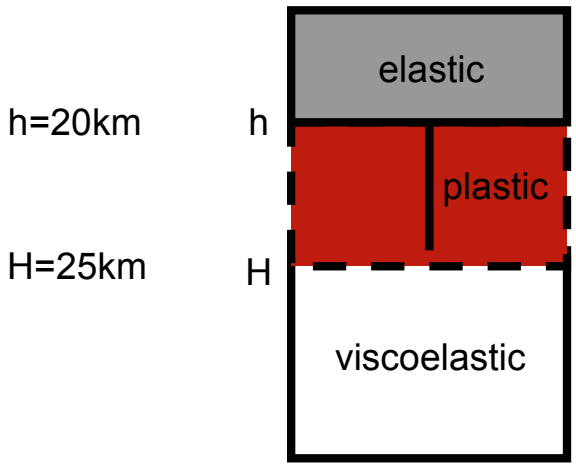

Adding poroelastic rebound improves data fit

Viscous model

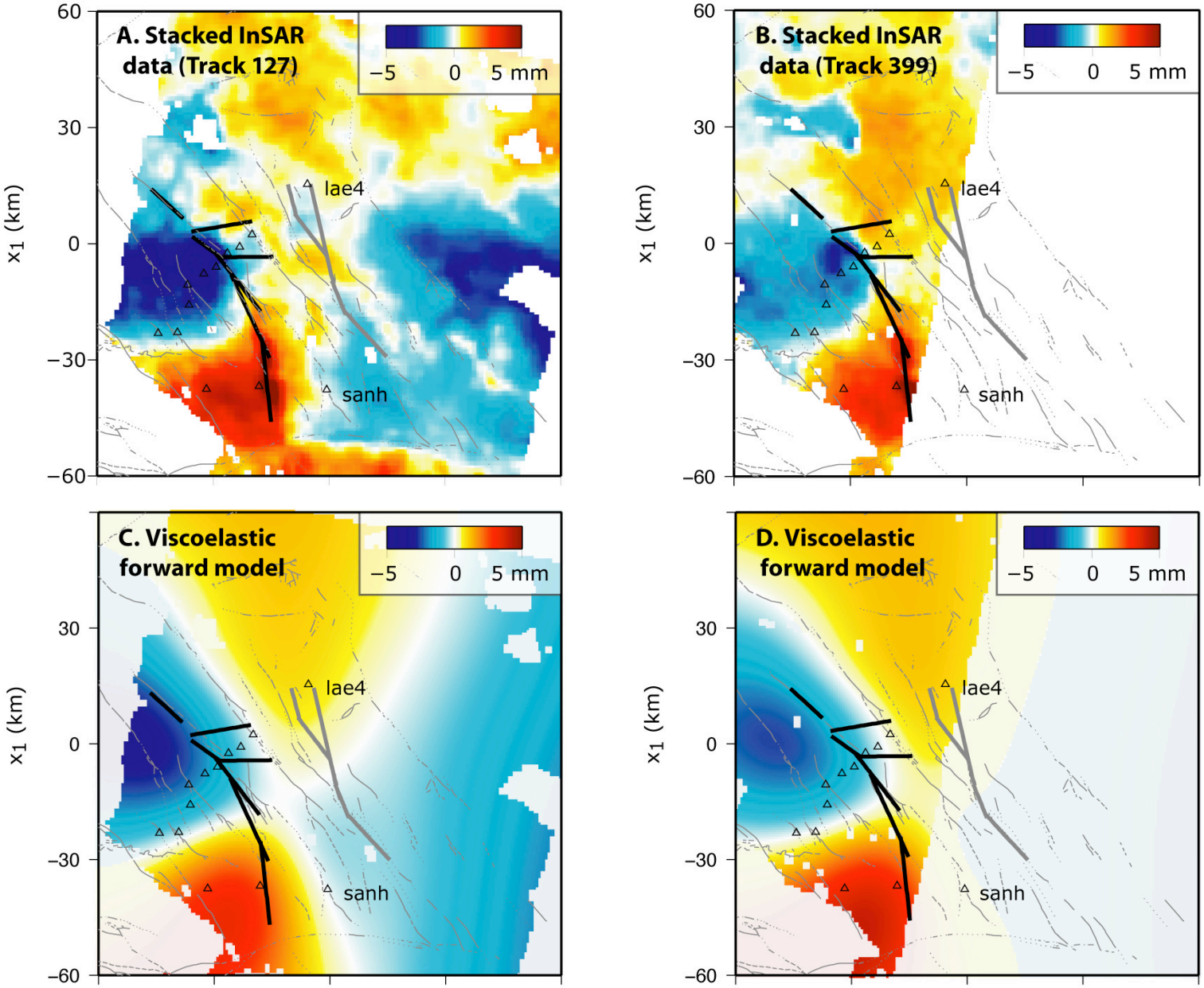

Viscous model

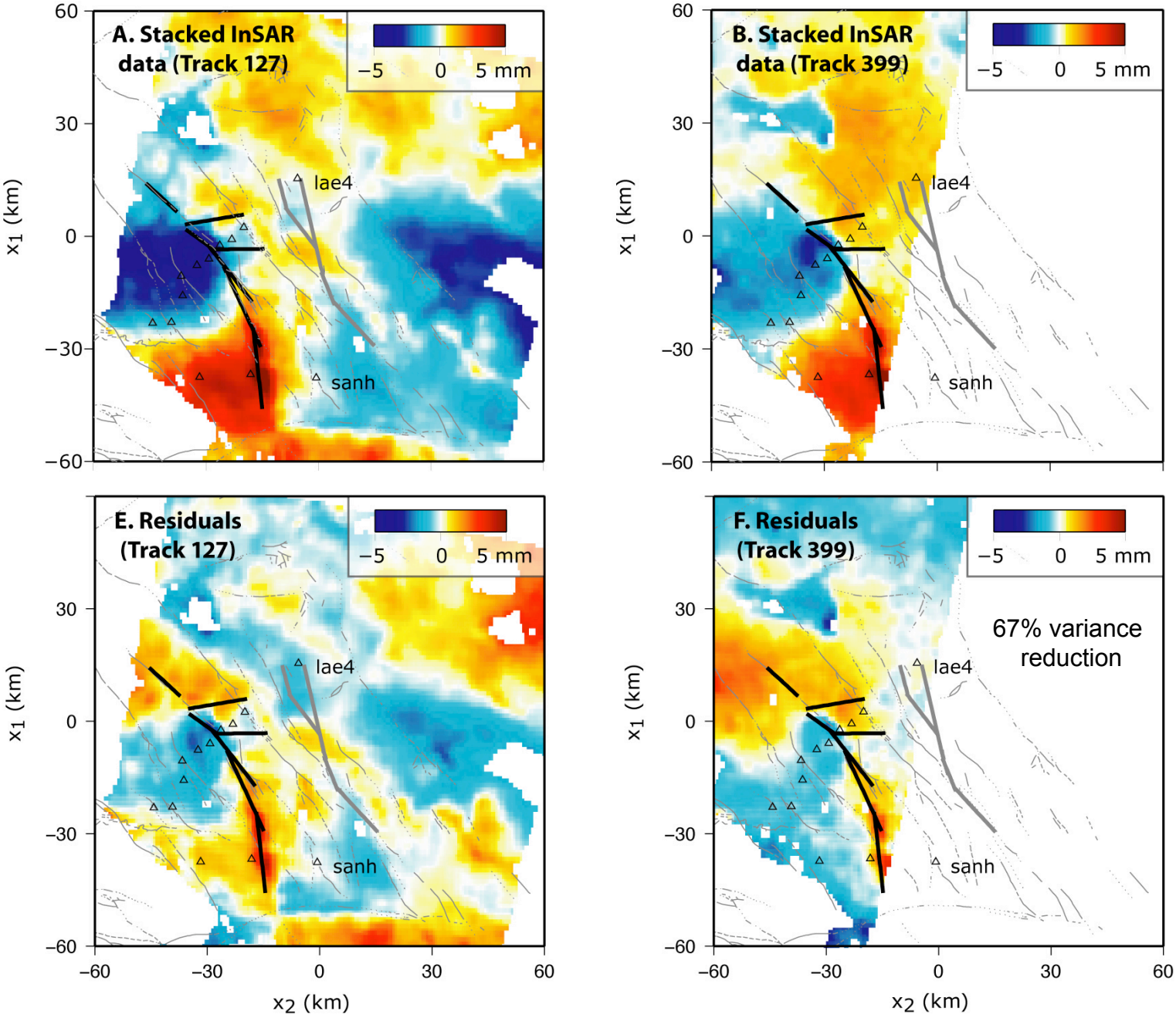

Lithosphere strength

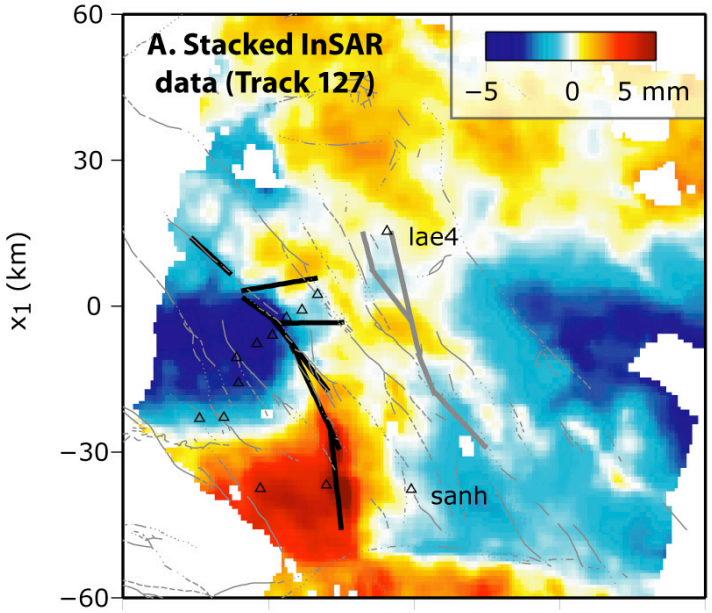

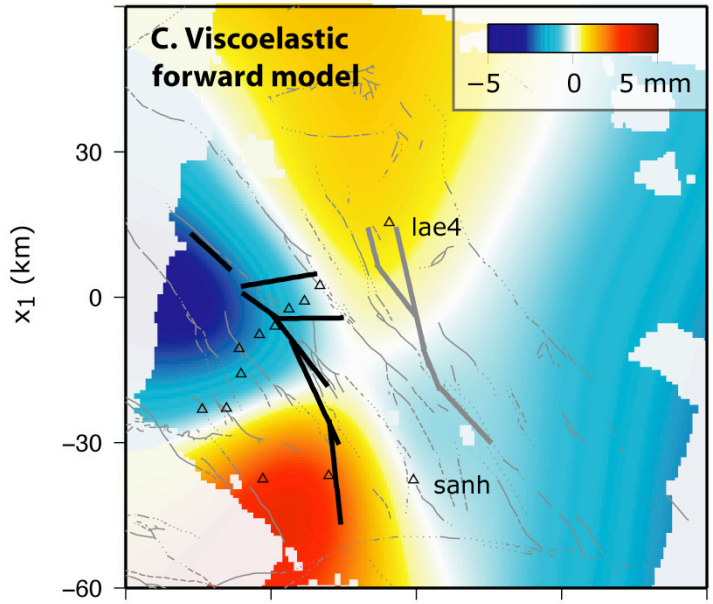

A. Models of lithosphere fluidity from post Landers InSAR data

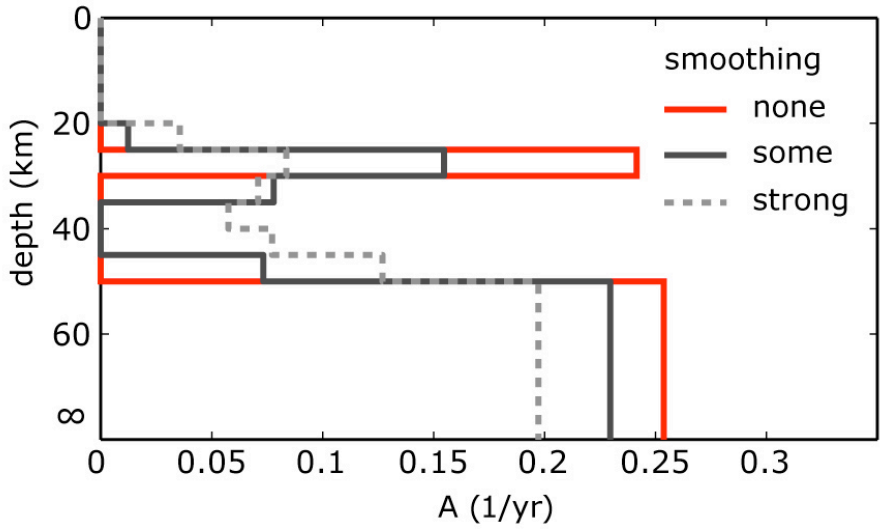

B. Inferred viscosity profile

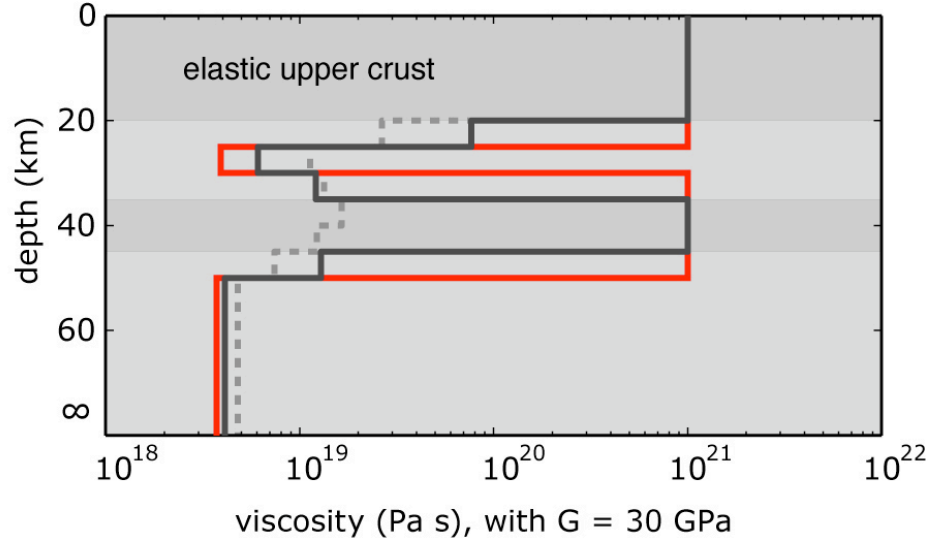

Lithosphere strength, effect of poroelasticity

A. Influence of poroelasticity on inferred fluidity

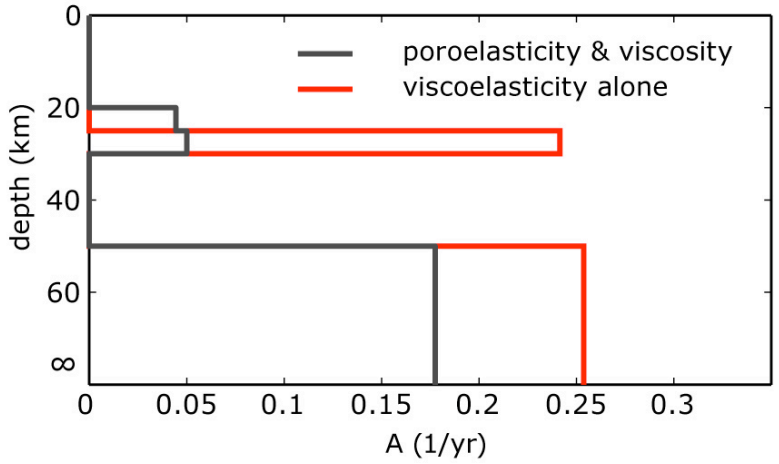

Joint poro- and viscoelastic model explains 71% of data

viscoelastic model explains 67% of data

B. Inferred viscosity profile (post-Landers InSAR data)

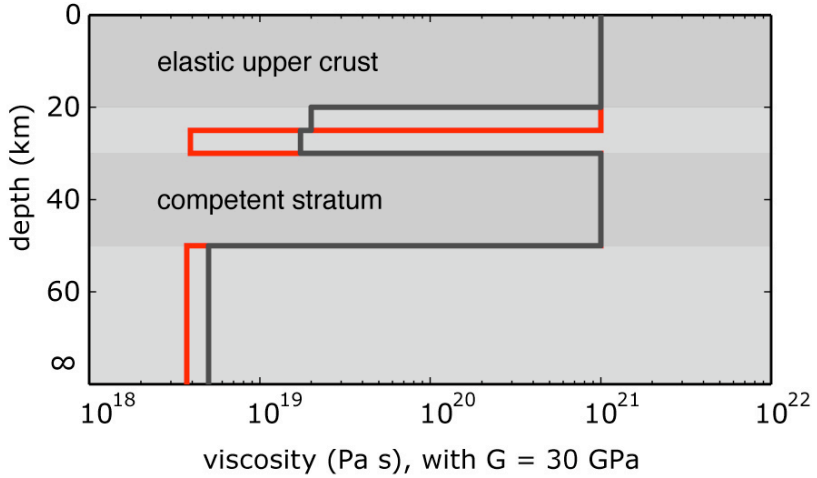

stratification of ductile layers is unaffected

Conclusions on Post-Landers modeling

- Preferred model is a combination of poroelastic rebound and viscoelastic flow with 71% variance reduction (VR)
- Second best model is viscoelastic flow alone (67% VR)
- A combination of afterslip and viscoelastic flow is a viable explanation of InSAR data (66% VR)
- Poroelastic rebound always improve quality of fit.

- Viscous flow likely takes place in two separate horizons, one between 25 and 30km depth another below 50km depth. Location of top layer may be biased up by the presence of afterslip.

Outlines

- Design of the linear inverse problem
- Models of post-Landers deformation with InSAR data
  - afterslip transitioning to viscous flow
  - poroelastic rebound & viscous flow
  - viscoelastic flow alone
- Resolution of geodetic data
- Models of post-Hector Mine deformation with InSAR and GPS data
  - poroelastic rebound & viscous flow
  - viscoelastic flow alone
- Lateral variations in viscosity
- Conclusions

Design of inverse problem: Landers & Hector Mine data set

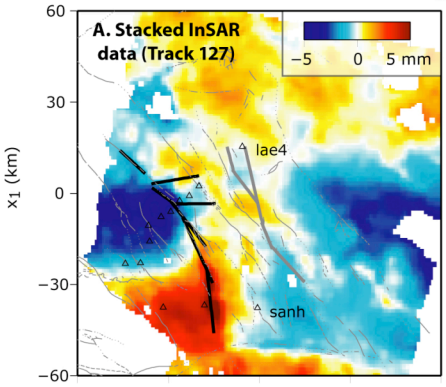

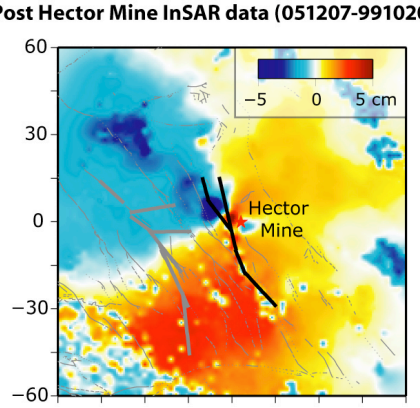

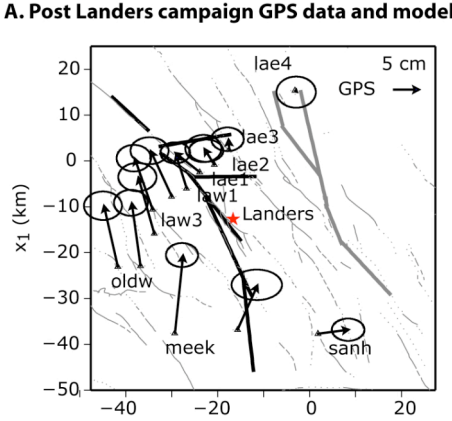

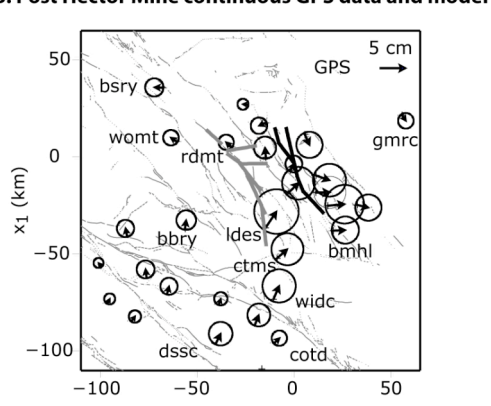

data vector

response of a nominal flow in horizon *i*

$$\mathbf{d} = \begin{bmatrix} d_1 \\ \vdots \\ d_N \end{bmatrix} \qquad \mathbf{G} = \begin{bmatrix} G_{11} & \cdots & \cdots & \cdots & \cdots & \cdots & G_{1M} \\ \vdots & & & & & & \vdots \\ G_{N1} & \cdots & \cdots & \cdots & \cdots & \cdots & G_{NM} \end{bmatrix} \qquad \mathbf{m} = \begin{bmatrix} m_1 \\ \vdots \\ m_M \end{bmatrix}$$

horizon *i*

Fit GPS time series

$$d(t) = m_1 + m_2(t - t_0) + m_3(1 - e^{-t/t_m})H(t - t_0) + m_4\cos(2\pi t) + m_5\sin(2\pi t) + m_6\cos(4\pi t) + m_7\sin(2\pi t)$$

Resolution of inverse problem: InSAR vs. GPS

spectral decomposition of the design matrix

$$\mathbf{G} = \mathbf{U}\Lambda\mathbf{V}^t$$

the misfit function can be written

$$\chi = \left\| \mathbf{U}^t\mathbf{d} - \Lambda\mathbf{V}^t\mathbf{m} \right\|$$

keep only large eigenvalues and define new design matrix

$$\tilde{\mathbf{G}} = \tilde{\Lambda}\mathbf{V}^t$$

infer the resolution on model parameters

$$\mathbf{R} = \tilde{\mathbf{G}}^t\left(\tilde{\mathbf{G}}\tilde{\mathbf{G}}^t\right)^{-1}\tilde{\mathbf{G}}$$

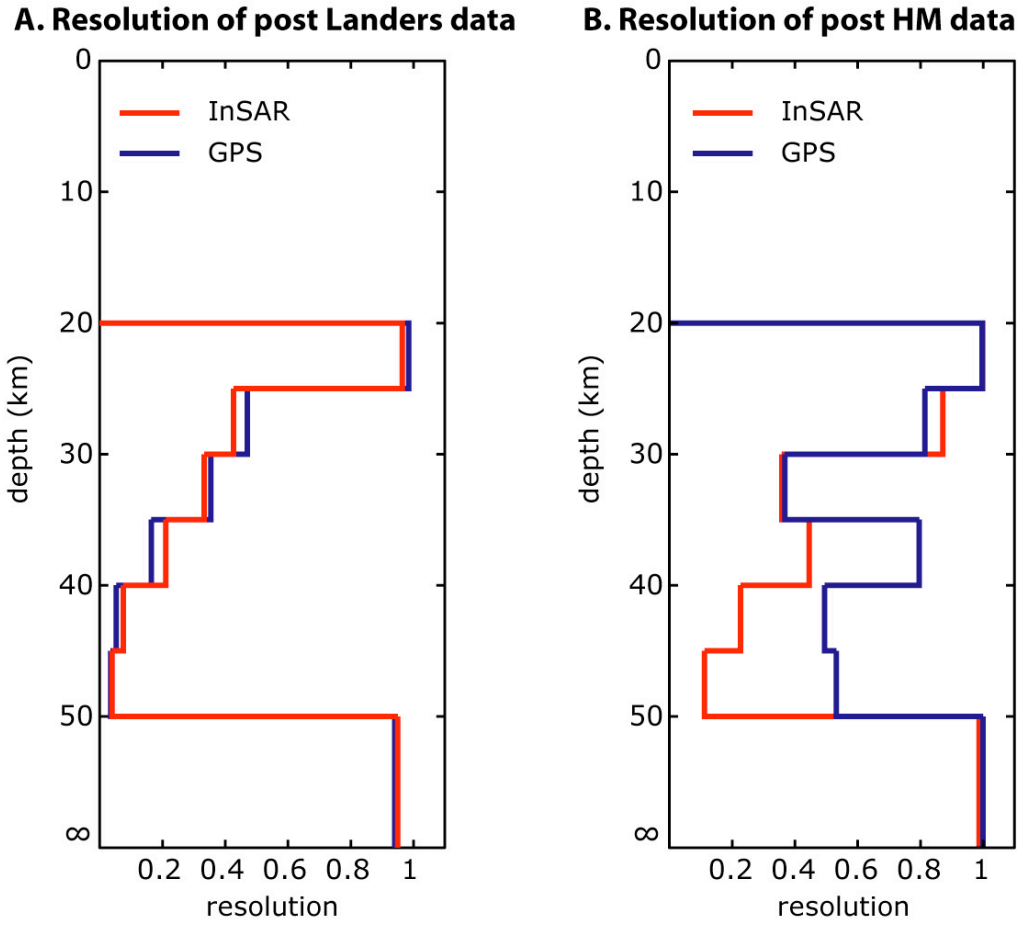

N=1600 data points
M=7 parameters

→ **under**-constrained inverse problem

Outlines

- Design of the linear inverse problem
- Models of post-Landers deformation with InSAR data
  - afterslip transitioning to viscous flow
  - poroelastic rebound & viscous flow
  - viscoelastic flow alone
- Resolution of geodetic data
- Models of post-Hector Mine deformation with InSAR and GPS data
  - poroelastic rebound & viscous flow
  - viscoelastic flow alone
- Lateral variations in viscosity
- Conclusions

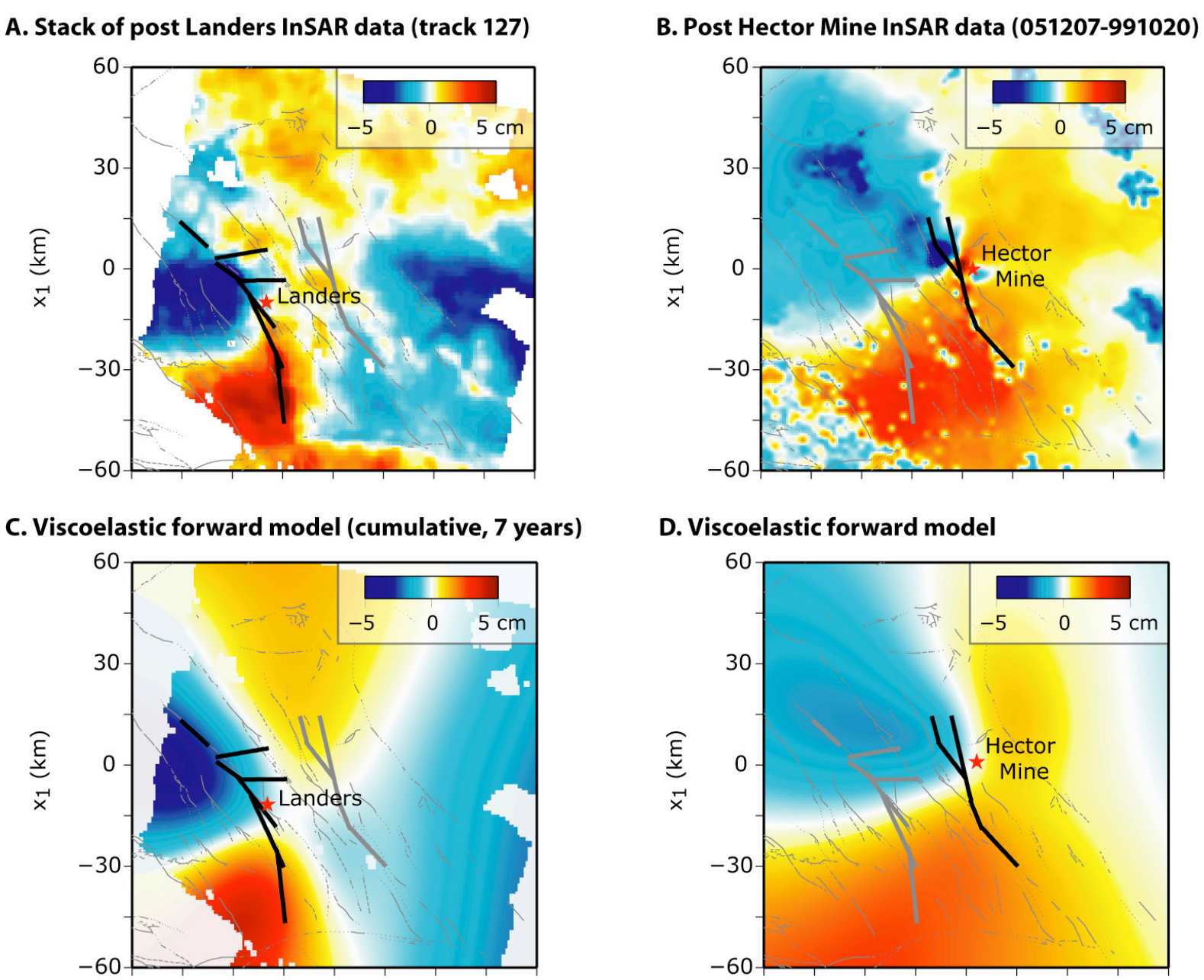
A. Stack of post Landers InSAR data (track 127)
B. Post Hector Mine InSAR data (051207-991020)
C. Viscoelastic forward model (cumulative, 7 years)
D. Viscoelastic forward model
60
30
0
−30
−60
x1 (km)
−5
0
5 cm
Landers
Hector
Mine

A. Stack of post Landers InSAR data (track 127)

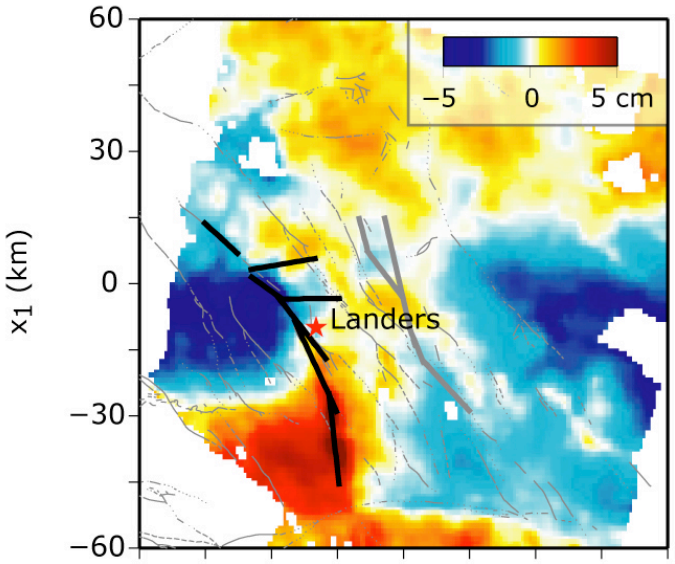

B. Post Hector Mine InSAR data (051207-991020)

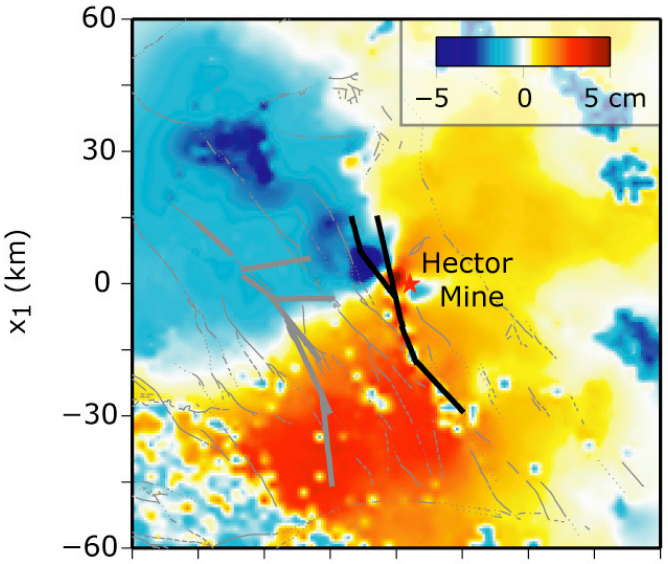

E. InSAR LOS residuals (post Landers)

67% variance reduction

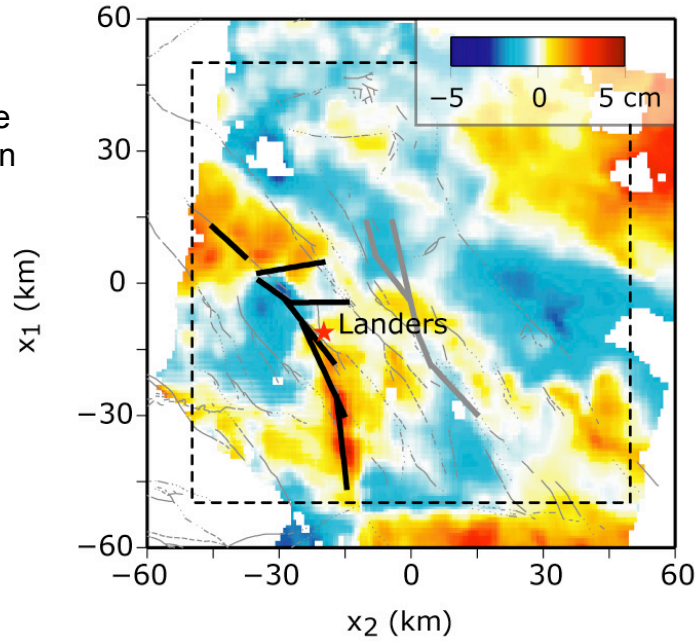

F. InSAR LOS residuals (post Hector Mine)

77.8% variance reduction

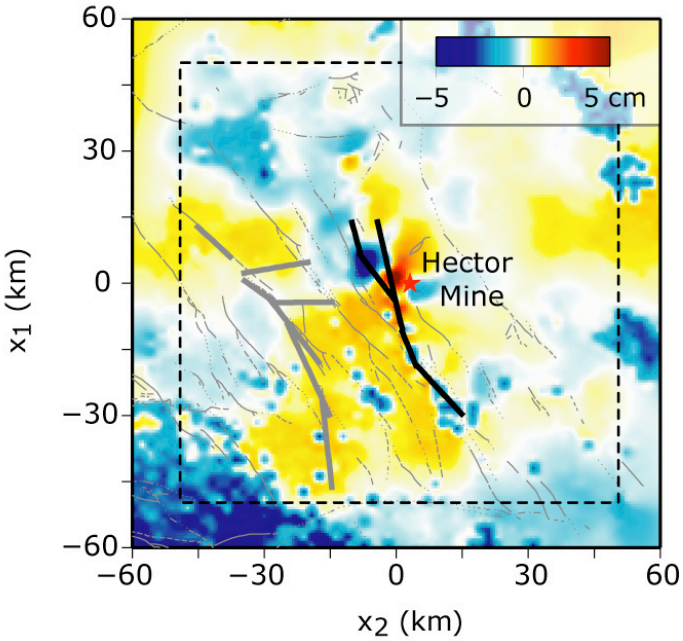

A. Post Landers campaign GPS data and model

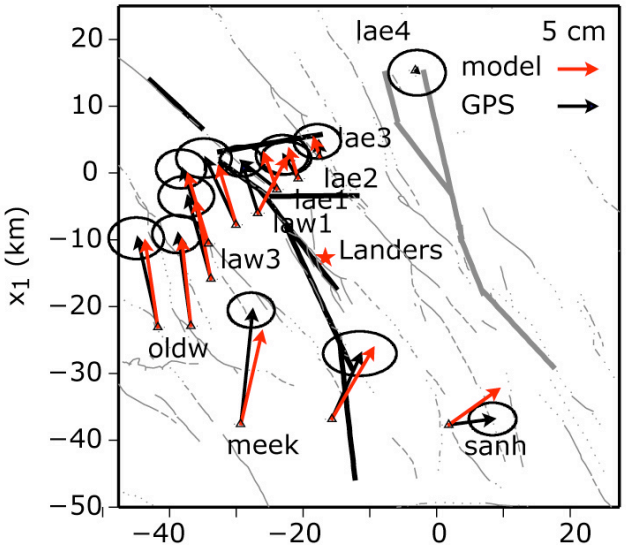

B. Post Hector Mine continuous GPS data and model

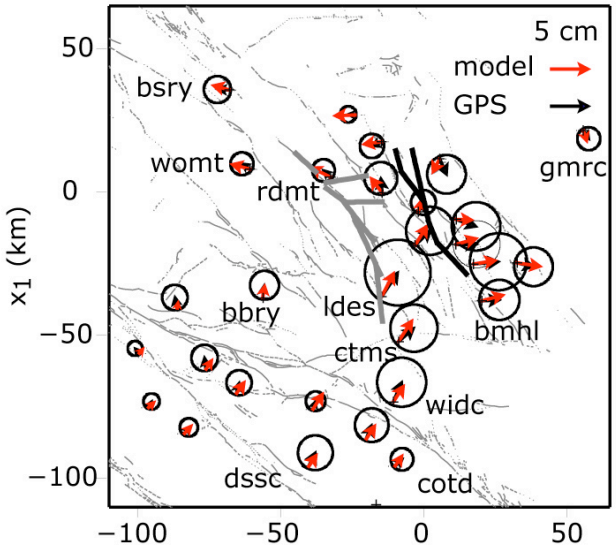

C. Residuals of post Landers viscoelastic model

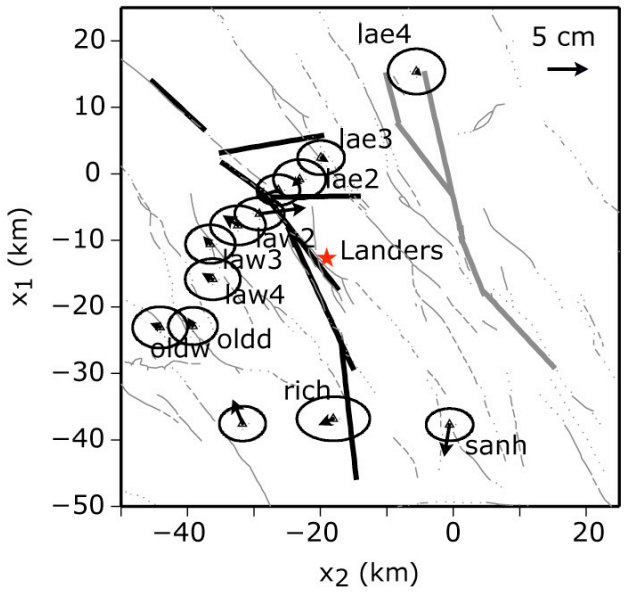

D. Residuals with post Hector Mine viscoelastic model

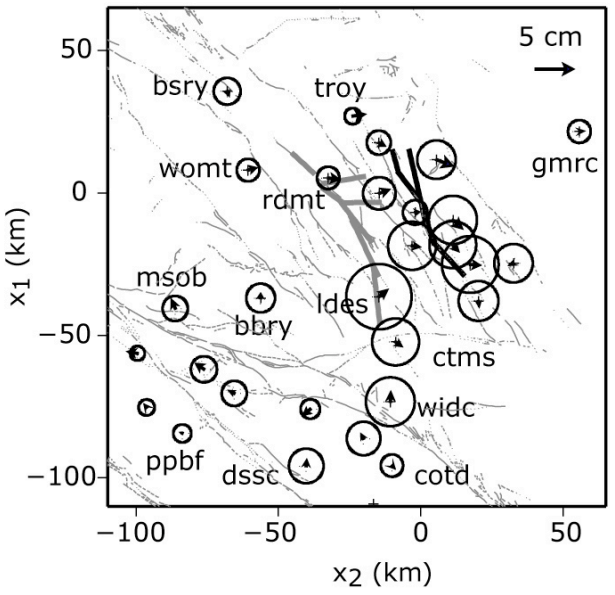

Time series: Landers

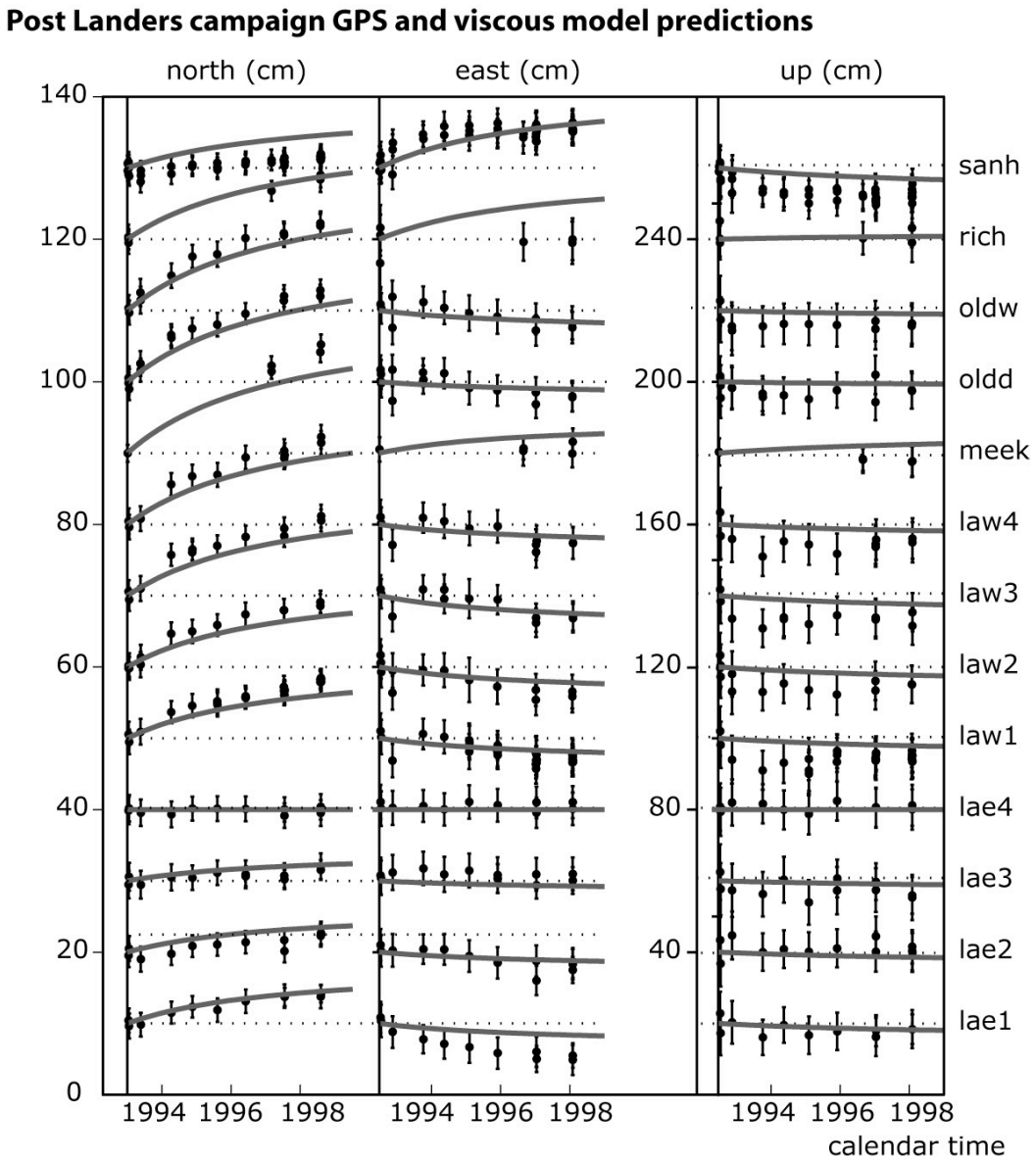

Time series: Hector Mine

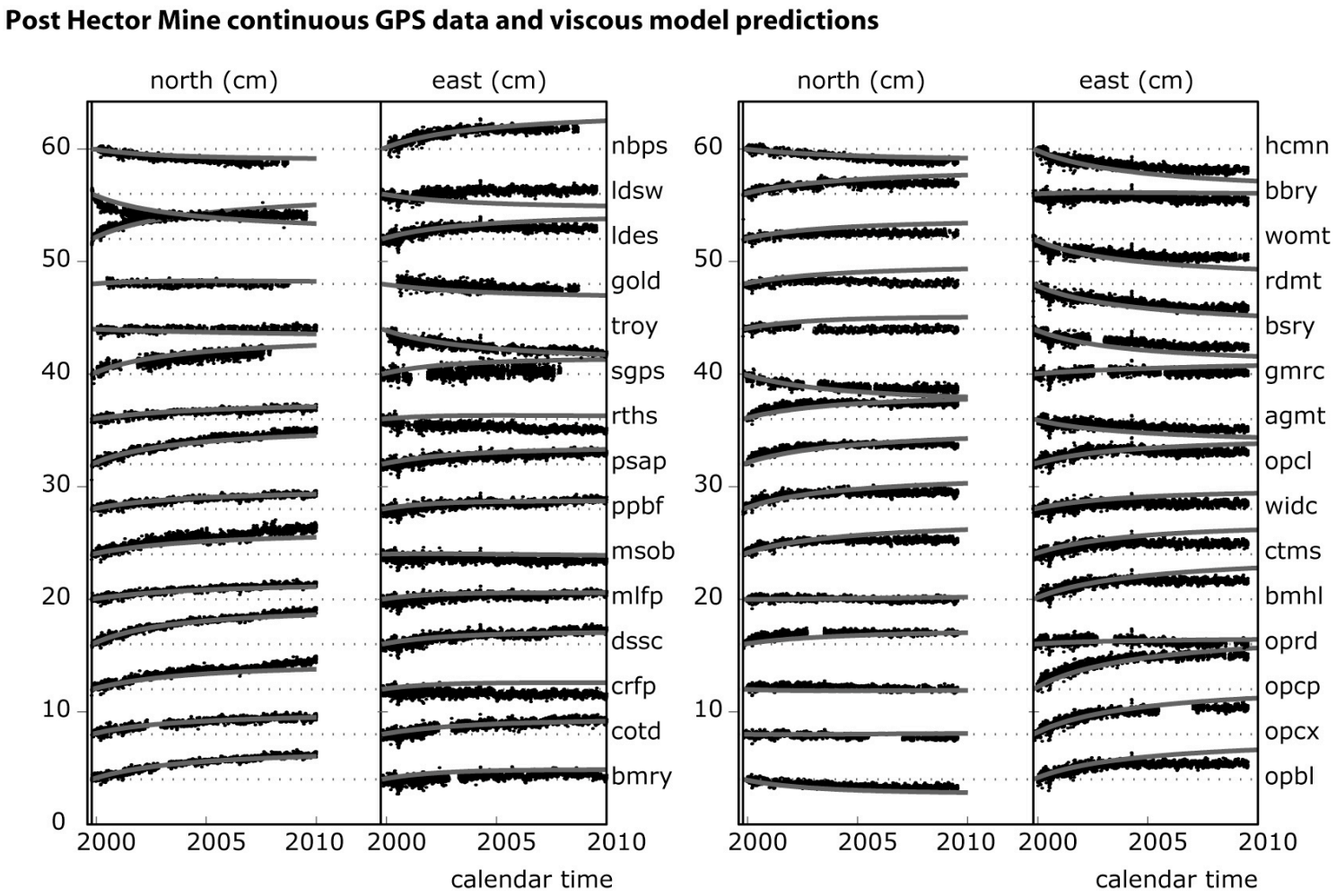

Preferred model and resolution

A. Models of lithosphere fluidity from post Landers and post HM data

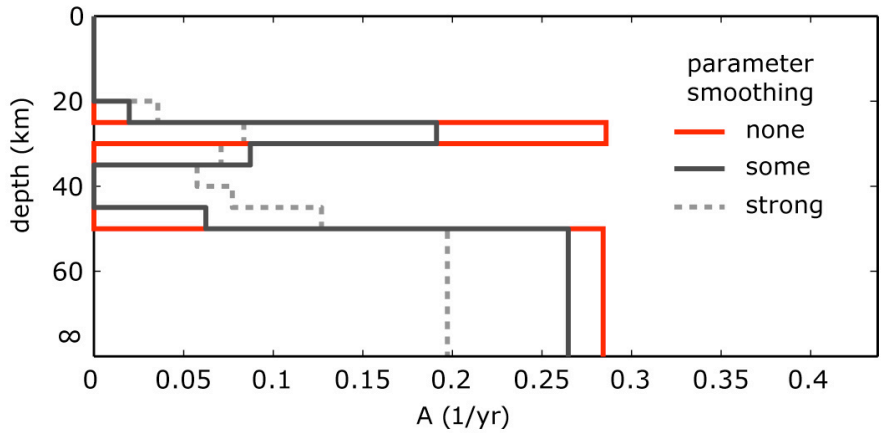

B. Inferred viscosity profiles

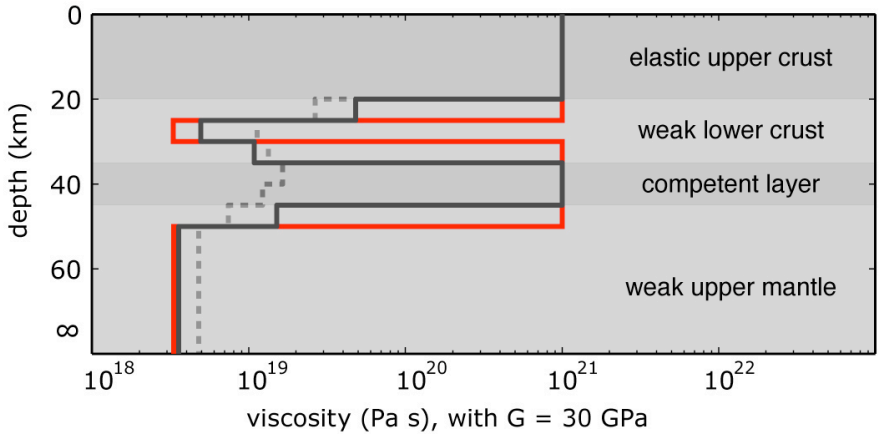

C. Resolution of inverse problem

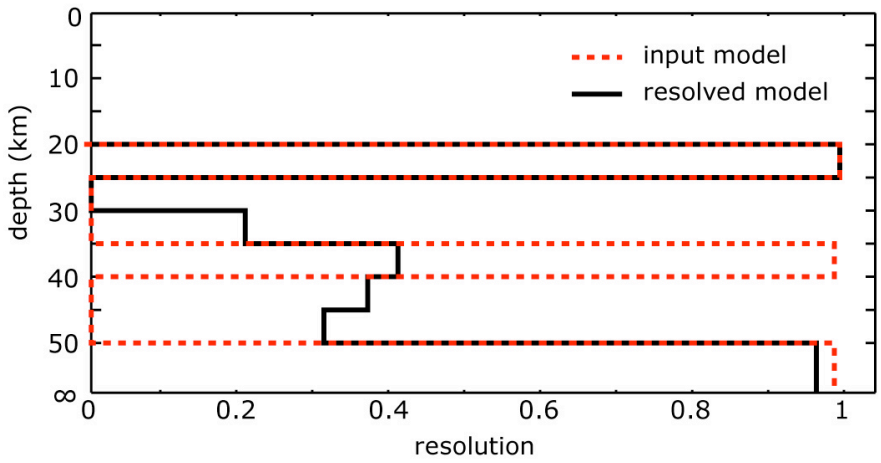

Geological implications

A. Models of lithosphere fluidity from post Landers and post HM data

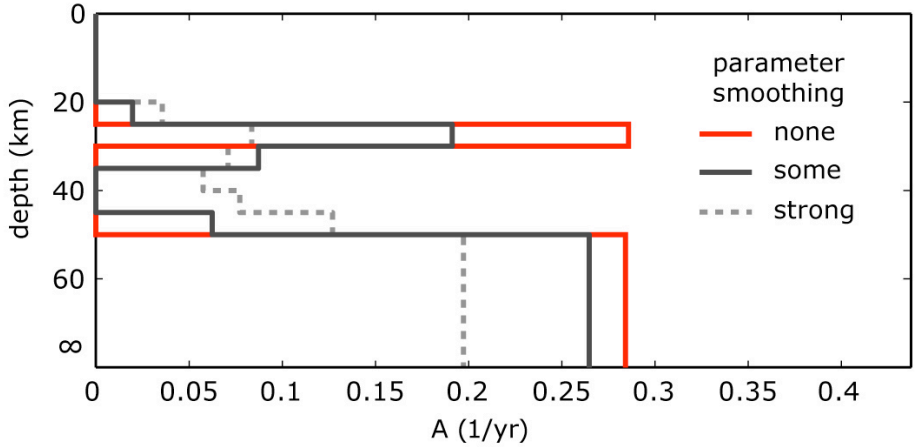

B. Inferred viscosity profiles

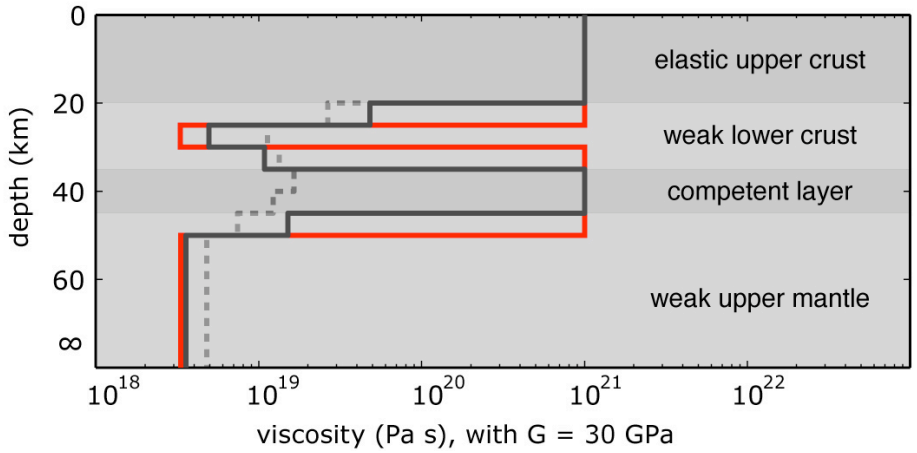

Depth of crust/mantle transition
(Moho)
in Southern California

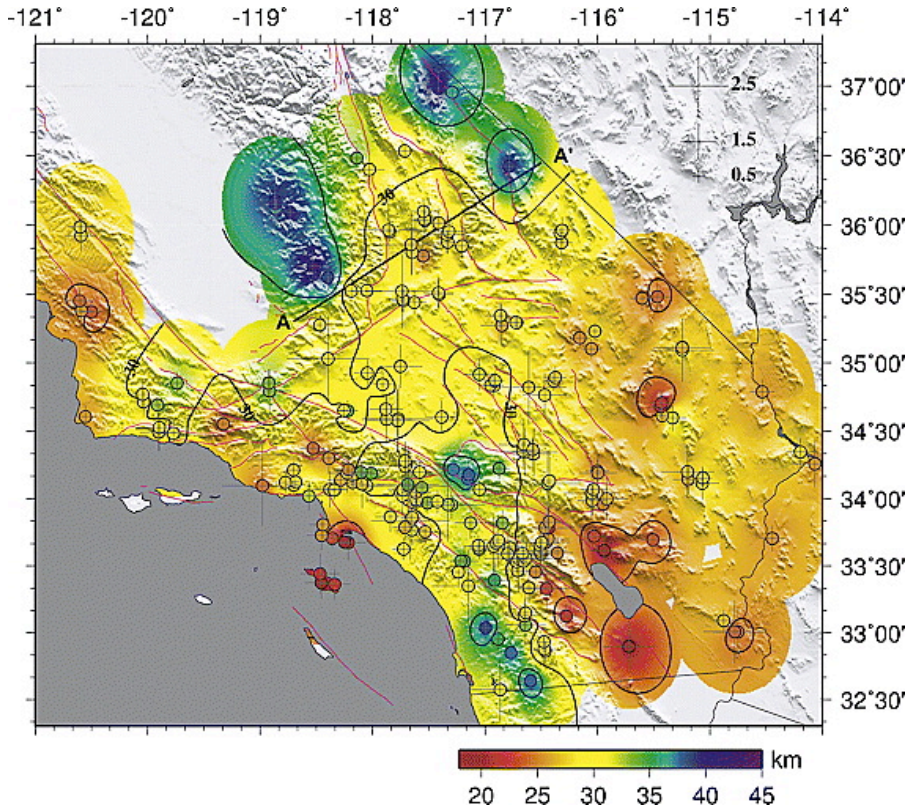

Yan & Clayton, 2007

Outlines

- Design of the linear inverse problem
- Models of post-Landers deformation with InSAR data
  - afterslip transitioning to viscous flow
  - poroelastic rebound & viscous flow
  - viscoelastic flow alone
- Resolution of geodetic data
- Models of post-Hector Mine deformation with InSAR and GPS data
  - poroelastic rebound & viscous flow
  - viscoelastic flow alone
- Lateral variations in viscosity
- Conclusions

3D tomography of lithosphere viscosity

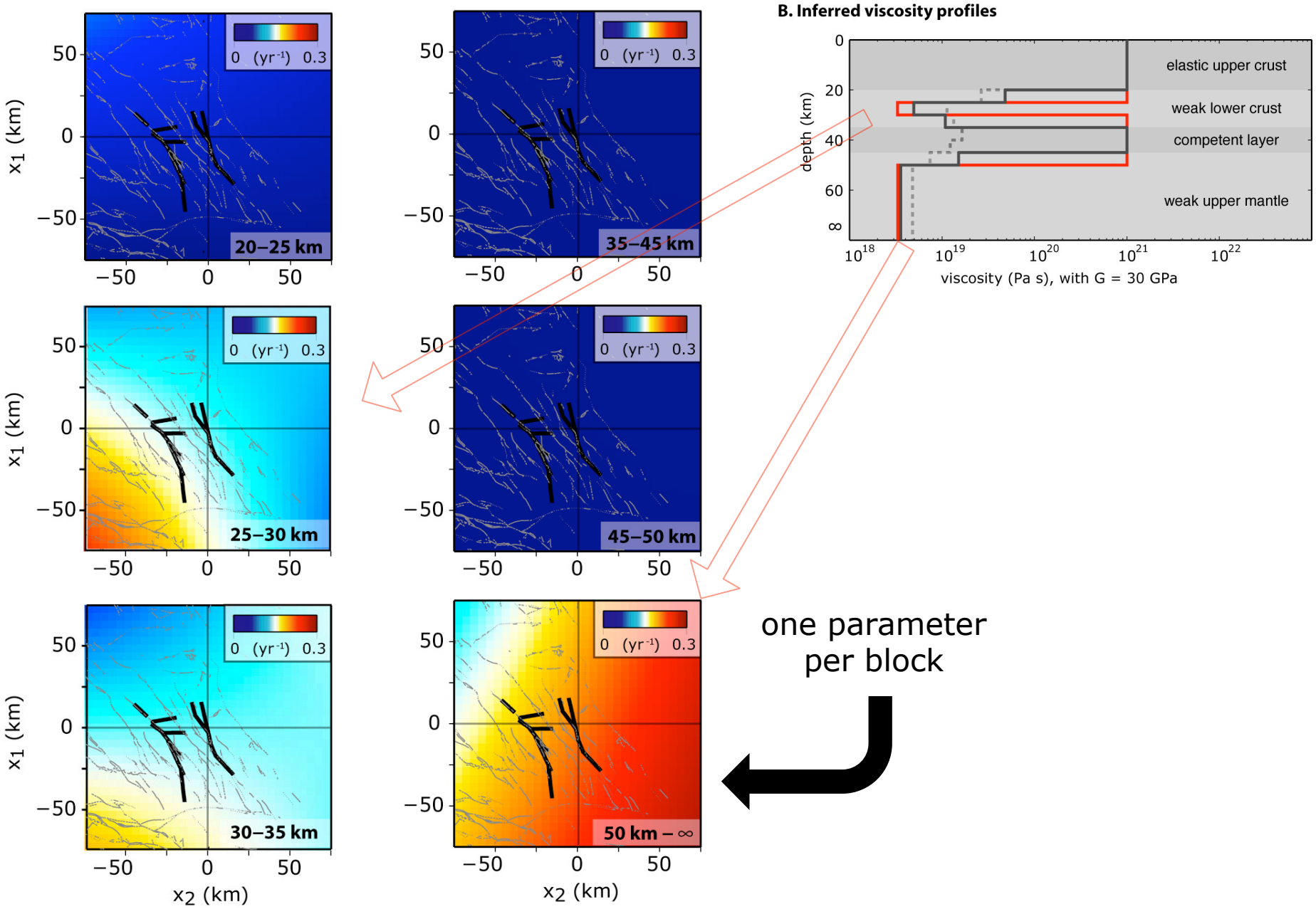

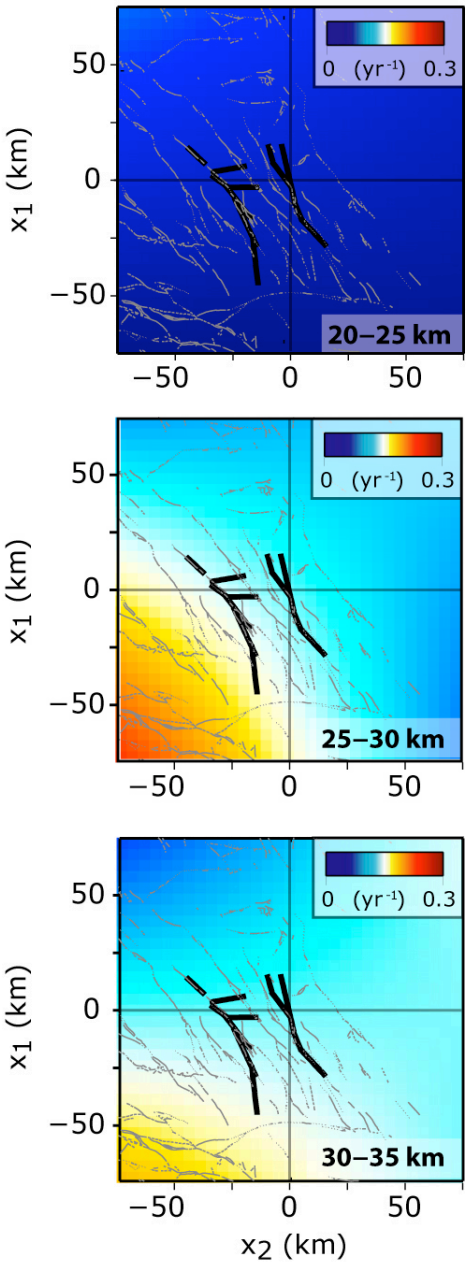

Thickness of ductile layer is coincident with deepening of Moho

Moho marks transition from crustal rocks to mantle rocks and ductile/competent transition

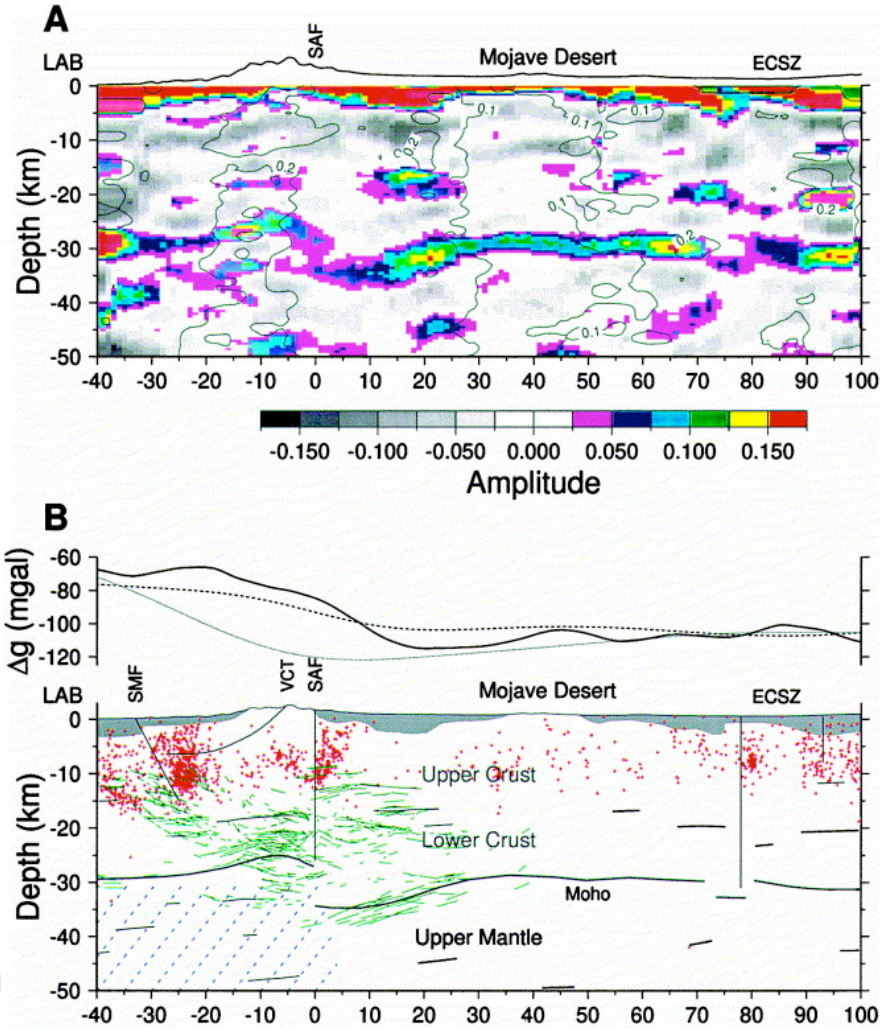

Zhu, 2000

Strength of the Mojave lithosphere

Zhu, 2000

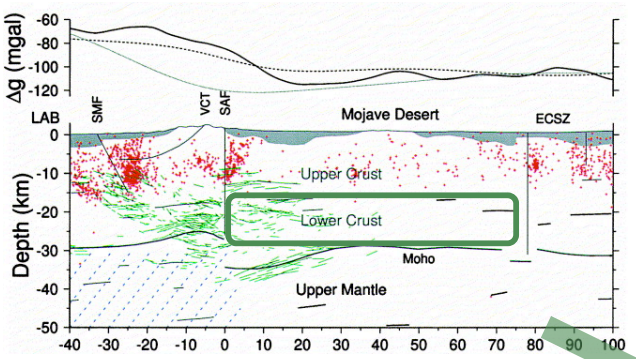

inferred
lower lithosphere fluidity

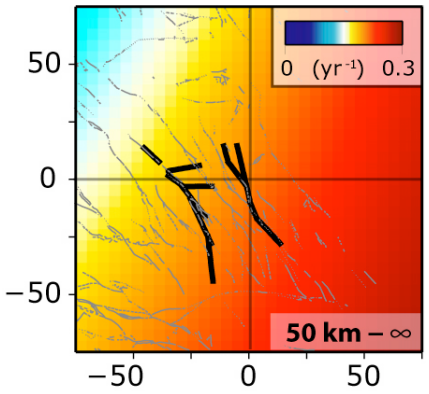

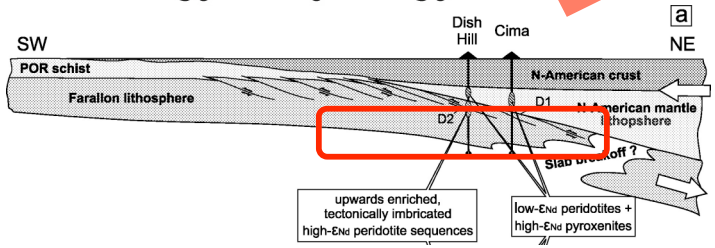

Luffi et al, 2009

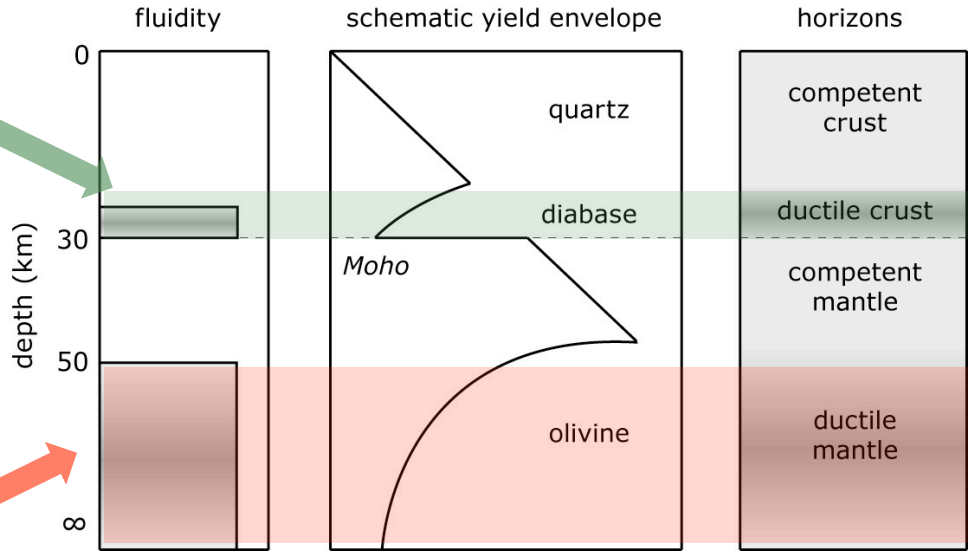

A tradeoff between poroelastic rebound and lower-crust viscous flow?

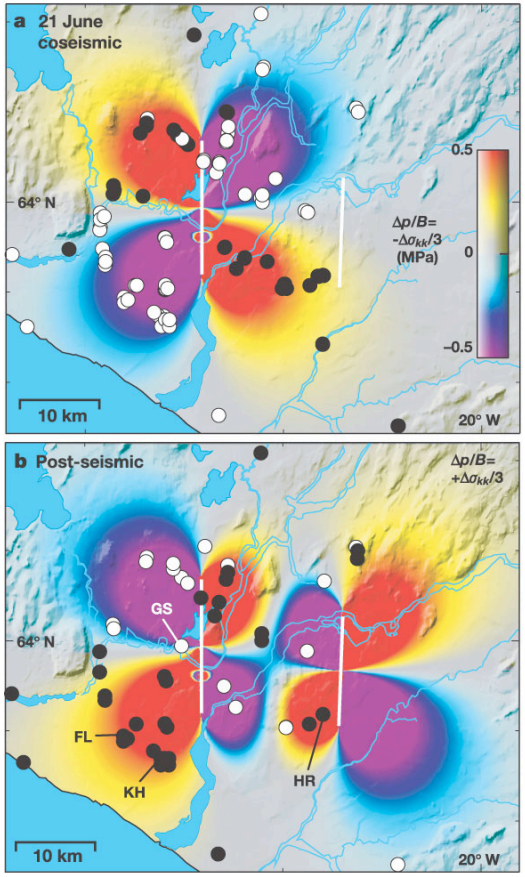

Jónsson et al., 2003

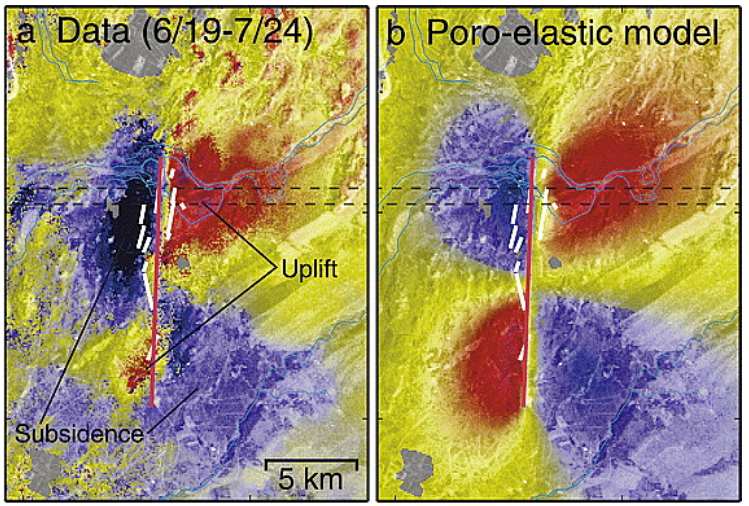

Árnadóttir et al., 2005

Is poroelastic rebound
a valid contributor to far-field
postseismic deformation?

Conclusions

- Afterslip is not a preferred model but may still take place (and bias inferred location of lower-crustal flow)
- The tradeoff between poroelasticity and viscoelasticity for the Landers data is resolved by the Hector Mine geodetic data
- Resolution of ductile horizons is greatly improved by considering Landers & Hector Mine data sets
- InSAR and GPS are best explained by the presence of two viscous horizons: the lower crust and the lower lithosphere separated by a mantle lid (jelly sandwich)
- Lateral variations in viscosity are more important in the lower crust than upper mantle.
- Mojave Moho marks transition between elastic AND viscous properties of rocks